

Dynamical Mean-Field Theory for Open Markovian Quantum Many Body Systems

Orazio Scarlatella,^{1,2} Aashish A. Clerk,³ Rosario Fazio,^{4,5} and Marco Schiró^{6,*}

¹*Clarendon Laboratory, University of Oxford, Parks Road, Oxford OX1 3PU, United Kingdom*

²*Institut de Physique Théorique, Université Paris Saclay, CNRS, CEA, F-91191 Gif-sur-Yvette, France*

³*Pritzker School of Molecular Engineering, University of Chicago, 5640 S. Ellis Ave., Chicago, IL, 60637, USA*

⁴*The Abdus Salam International Centre for Theoretical Physics, Strada Costiera 11, I-34151 Trieste, Italy*

⁵*Dipartimento di Fisica, Università di Napoli “Federico II”, Monte S. Angelo, I-80126 Napoli, Italy[†]*

⁶*JEIP, USR 3573 CNRS, Collège de France, PSL Research University,
11, place Marcelin Berthelot, 75231 Paris Cedex 05, France*

(Dated: June 6, 2022)

Open quantum many body systems describe a number of experimental platforms relevant for quantum simulations, ranging from arrays of superconducting circuits hosting correlated states of light, to ultracold atoms in optical lattices in presence of controlled dissipative processes. Their theoretical understanding is hampered by the exponential scaling of their Hilbert space and by their intrinsic nonequilibrium nature, limiting the applicability of many traditional approaches. In this work we extend Dynamical Mean Field Theory (DMFT), a powerful nonperturbative technique developed for strongly correlated quantum many-body systems, to Markovian open quantum systems. Within Open-DMFT, a master equation describing a lattice of bosonic particles is mapped, at large but finite connectivity, onto an impurity problem describing a single site coupled to Markovian and non-Markovian environments, where the latter accounts for quantum fluctuations beyond Gutzwiller mean-field theory. We introduce a new non-perturbative approach to solve the impurity problem, which dresses the impurity, featuring Markovian dissipative channels, with the non-Markovian bath, in a self-consistent scheme based on a resummation of non-crossing diagrams. Finally, we apply our Open-DMFT to solve a driven-dissipative Bose-Hubbard model, which is relevant to current experiments with dissipative ultracold bosons. We show that this model undergoes a dissipative phase transition towards a superfluid phase, which can be equally interpreted as a quantum many-body synchronization transition of an array of quantum van der Pol oscillators. We show how Open-DMFT captures crucial effects due to finite lattice connectivity, such as hopping-induced dissipation and heating, which are completely missed by mean field theories and which lead to a drastic reduction of the broken symmetry phase that we interpret as a desynchronization driven by quantum fluctuations.

I. INTRODUCTION

Developments in quantum science and quantum engineering have brought forth a variety of platforms to store, control and process information at genuine quantum levels. Examples include trapped atoms and ions [1], quantum cavity-QED systems [2], superconducting qubits [3] or quantum optomechanical systems [4]. These architectures are not only of great relevance for quantum technologies but also for the quantum simulation of emergent collective many-body phenomena. We now have several experimental quantum simulators worldwide running on a variety of architectures, from ultracold atoms in optical lattices [5], Rydberg gases [6], trapped ions [7] and coupled cavity arrays [8]. Such simulators have led to significant advances in our understanding of quantum many-body phases and offer us an opportunity to address deep unanswered questions concerning the behavior of quantum matter in novel unexplored regimes, particularly far away from thermal equilibrium.

Many of these systems are typically characterized by

excitations with a finite lifetime, due to unavoidable losses, dephasing and decoherence processes originating from their coupling to external environments and therefore feature an intrinsic nonequilibrium nature. Arrays of circuit QED cavities, for example, are emerging as a unique platform for the quantum simulations of driven-dissipative quantum many body systems [8–11], where the balance of drive and loss processes and the presence of strong non-linearities, allows one to reach interesting non-equilibrium stationary states. Experiments have recently started to show a variety of dissipative quantum phases and phase transitions [12–15]. This includes the recent experimental realization of a dissipatively stabilised Mott insulator [16]. On a different front, recent advances with ultracold atoms in optical lattices allow the engineering of controlled dissipative processes, such as correlated losses [17, 18] or heating due to spontaneous emission [19, 20] and to study the resulting quantum many body dynamics over long time scales. These experimental settings offer fresh new inputs for quantum simulations of strongly correlated driven-dissipative quantum many-body systems, at the interface between quantum optics and condensed matter physics [21–26].

From a theoretical standpoint these experimental platforms can be well described as open Markovian quantum systems, of either fermionic/bosonic particles or quan-

* On Leave from: Institut de Physique Théorique, Université Paris Saclay, CNRS, CEA, F-91191 Gif-sur-Yvette, France

[†] On leave

tum spins, evolving through a Lindblad master equation for the many body density matrix ρ [27]. The crucial aspect of this problem lies in the interplay between unitary dynamics and the dissipative evolution, out of which non trivial stationary states can be engineered [28–31]. Open Markovian quantum many body systems are predicted to display a broad range of new transient dynamical phenomena [32–35] and dissipative quantum phase transitions [36–41].

Solving the Lindblad equation for many-body systems is extremely challenging. Exact numerical solutions based on the diagonalization of the Lindbladian superoperator, or direct time evolution, are limited to very small systems, and only slightly larger systems can be addressed with quantum trajectories [42]. For one dimensional systems an efficient representation of the problem in the language of matrix product operator is possible [43, 44] and has been successfully used in the recent past [45], however its extension to higher dimensional systems poses problems, although some recent results have been obtained [46, 47]. As a result a number of theoretical approaches have been developed in recent years to tackle driven-dissipative lattice systems [47–58].

Driven-dissipative correlated bosons, such as those described by Bose-Hubbard and related models, are particularly challenging to tackle numerically due to the unbounded Hilbert space. Most theoretical approaches are limited to quantum spin models, or to solely describe static correlations encoded in the stationary state density matrix. In contrast many experimental platforms operate beyond the two-level approximation and are naturally sensitive to finite frequency probes related to dynamical correlations functions.

These experimental achievements and theoretical challenges motivate this work, whose main results are the following ones:

(I) We formulate a novel approach to open Markovian bosonic quantum many-body systems, by extending the dynamical mean field theory (DMFT) of correlated electrons [59] and bosons [60, 61] to the realm of open Markovian quantum systems. DMFT is a powerful non-perturbative technique based on the large lattice connectivity limit [62, 63] which has been successfully applied to a variety of nonequilibrium fermionic problems [64], including non-linear transport within an auxiliary Lindblad master equation [65] and to study unitary dynamics of correlated bosons [66]. Our Open-DMFT maps the original Lindblad master equation onto a quantum impurity problem, describing a single lattice site, which in our case features an interacting bosonic mode in presence of Markovian drive and dissipation, embedded in a self-consistent non-Markovian environment. Solving such a quantum impurity model, although simpler than the full lattice, remains highly non trivial.

(II) We introduce a new diagrammatic approach to solve the quantum impurity model which fully captures the underlying Markovian dynamics and accounts for the non-Markovian bath through the resummation of an in-

finite class of diagrams in the impurity-bath coupling known as non-crossing approximation (NCA).

(III) Using Open-DMFT we study a prototypical Markovian quantum many-body system, a Bose-Hubbard model subject to two-particle losses and single particle incoherent pumping. This model is directly relevant for recent experiments with ultracold bosonic atoms in optical lattices under controlled dissipation [18, 20]. We predict the emergence of a dissipative phase transition from a normal to a superfluid phase, where above a critical hopping or drive strength the system spontaneously develops a coherent field oscillating in time, and discuss the effect of accounting for quantum fluctuations beyond mean-field. We highlight how this transition can be naturally interpreted as the onset of many body synchronization in an array of quantum Van der Pol oscillators, a phenomenon which recently attracted lots of attention [67–79].

The paper is organized as follows. In the next section II we summarize of the main results of this work. In Sec. III we present the main aspects of the Open-DMFT method and discuss its physical content. In Sec. IV we discuss two methods to solve the quantum impurity problem: a strong coupling perturbative approach and a more powerful self-consistent NCA method. In Sec. V we present our results for an interacting Bose-Hubbard driven-dissipative lattice problem. Sec. VI is devoted to conclusions. In the Appendixes we provide technical details on the derivation of Open-DMFT (Appendix A), a non trivial consistency check on the NCA approximation (Appendix B) and various analytical results quoted in the main text (Appendixes C-D).

II. SUMMARY OF MAIN RESULTS

In this section we present a summary of the main results of this work, which will be discussed more in detail in the rest of the paper. In particular in Sec. IIA we discuss the formulation of Open-DMFT and of the NCA impurity solver while in Sec. IIB we present the application to a driven-dissipative Bose-Hubbard model.

A. Open Dynamical Mean-Field Theory

The class of models that we address with the Open-DMFT approach describe driven-dissipative bosonic particles on a lattice with coordination number z , whose coherent evolution is governed by the Hamiltonian

$$H = -\frac{J}{z} \sum_{\langle ij \rangle} \left(b_i^\dagger b_j + \text{hc} \right) + \sum_i H_{loc}[b_i^\dagger, b_i]. \quad (1)$$

Here $[b_i, b_i^\dagger] = 1$ are bosonic modes localized around the lattice site i , coupled together by a nearest-neighbours hopping term J . $H_{loc}[b_i^\dagger, b_i]$ is a generic local Hamiltonian, which can contain arbitrary local interactions. In

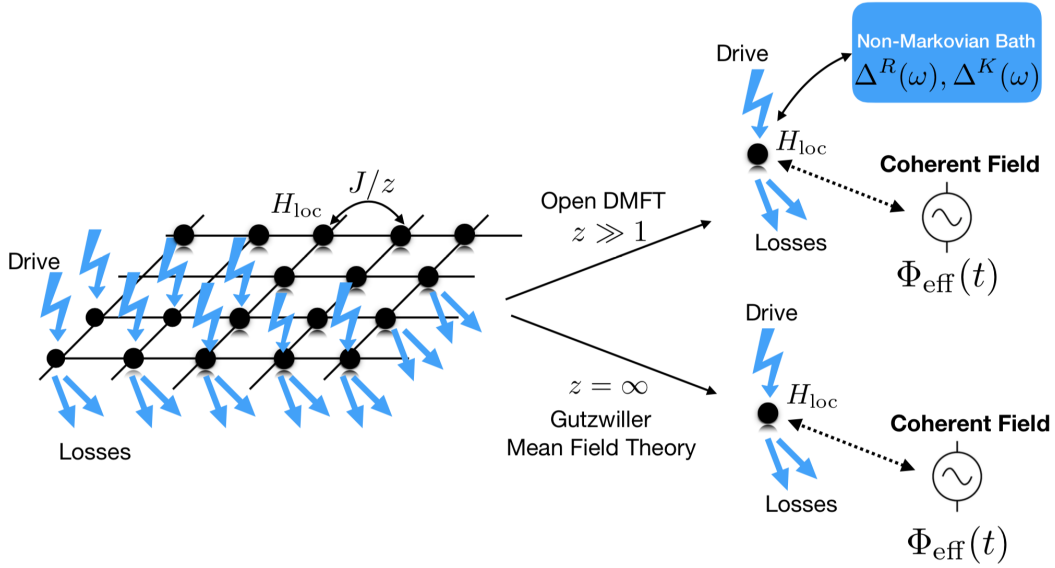


FIG. 1. Sketch of the Open-DMFT mapping for open Markovian quantum systems. A lattice of interacting, driven-dissipative bosons coupled by hopping (left, see Eq. (1-2) in the main text) is mapped in the large connectivity limit $z \gg 1$ onto a single site problem, with interactions, local Markovian drive and losses, coupled to a self-consistent environment (right, top panel). This includes a coherent drive and a non-Markovian bath (with its spectrum $\Delta^R(\omega)$ and distribution function $\Delta^K(\omega)$) which accounts for quantum fluctuations due to neighboring sites. In the infinite coordination limit, $z = \infty$, one recovers the Gutzwiller mean-field theory (right, bottom panel), where the effect of the lattice is simply encoded in a self-consistent field.

order for the problem to remain well defined in the limit of infinite connectivity $z \rightarrow \infty$, to which we will compare our Open-DMFT results, we scale the hopping with a $1/z$ factor, as usually done for bosons [60, 61, 80] (see also Sec. III A for further details). Although in this paper we focus on bosonic models, it is important to remark that Open-DMFT can be also applied to fermions and spins.

The many-body density matrix of the system evolves according to a Lindblad master equation with a set of local jump operators for each lattice site $L_{i\mu}$, accounting for dissipative processes, i.e.

$$\partial_t \rho = -i[H, \rho] + \sum_{i\mu} \left(L_{i\mu} \rho L_{i\mu}^\dagger - \frac{1}{2} \{ L_{i\mu}^\dagger L_{i\mu}, \rho \} \right). \quad (2)$$

The Open-DMFT approach considers the master equation (2) in the limit of large, but finite, lattice connectivity $z \gg 1$. In fact, when the number of neighbors z of a given lattice site is large, statistical and quantum fluctuations induced by the neighboring sites get small and can be treated in an approximate way, while the local, on-site physics is accounted for exactly. As we discuss in detail in Sec. III, in the $z \gg 1$ limit the Lindblad lattice problem formally maps onto a quantum impurity model describing an interacting Markovian single-site, characterized by the same local Hamiltonian H_{loc} and local jump operators $L_{i\mu}$ entering Eq. (2), coupled to a coherent driving field $\Phi_{eff}(t)$ and a non-Markovian, frequency dependent, quantum bath (Fig. 1, top panel). These take into account the effect of the neighboring sites and have to be determined self-consistently. As a result of the non-equilibrium nature of the problem, the non-Markovian environment is

described in terms of both its spectrum *and* distribution, encoded in the retarded $\Delta^R(\omega)$, and Keldysh $\Delta^K(\omega)$ hybridization functions of the bath, which for a generic non-equilibrium condition are independent and not related by the fluctuation-dissipation theorem.

To appreciate the physical content of Open-DMFT it is instructive to compare it with the widely used Gutzwiller mean-field theory, which we will show in Sec. III A to coincide with the $z \rightarrow \infty$ solution of the many-body master equation. This mean-field theory amounts to decouple the hopping term in the Hamiltonian (1), or equivalently assumes a product-state density matrix over different lattice sites, thus reducing the full many-body problem to a single site coupled to a self-consistent coherent field (Fig. 1, bottom panel). An obvious shortcoming of the Gutzwiller approach is that it cannot capture any coherent or dissipative processes arising from the coupling to neighboring sites, unless the system is in a broken-symmetry phase with a non-vanishing local order parameter, leading to a finite self-consistent field. The result is a particularly poor description of strongly interacting, yet incoherent, normal phases such as bosonic Mott insulators whose local properties within Gutzwiller are completely independent on the hopping and identical to those of an isolated site. In this perspective Open-DMFT accounts, non perturbatively, for the leading $1/z$ corrections to Gutzwiller mean field theory, capturing quantum fluctuations induced by the neighboring sites even in absence of an order parameter, through the non-Markovian bath.

Although simplified with respect to the full master

equation, the solution of the Open-DMFT equations and in particular of the quantum impurity problem sketched in Figure 1 still poses tremendous challenges due to the simultaneous presence of local interactions, Markovian drive and dissipation and non-Markovian bath. A major result of this paper is the introduction of a new non-perturbative method to solve this impurity problem, based on a self-consistent expansion in the non-Markovian bath and on a resummation of non-crossing diagrams, recently developed in Ref. [81]. As we will discuss further on in the paper, the self-consistent nature of the non-crossing approximation (NCA) we use, as opposed to bare perturbative expansions to which we will compare our results, is crucial to fully capture the non-trivial correlations associated to the Open-DMFT bath.

We give a more complete picture of the Open-DMFT formalism, including a discussion of the basic equations and of impurity solvers in Sec. III and Sec. IV.

B. Application to a Driven-Dissipative Bose Hubbard Lattice

In this work, we apply Open-DMFT to a lattice model of driven-dissipative interacting bosons by specifying the local Hamiltonian and local jump operators entering Equations (1-2). We consider for the former

$$H_{\text{loc}} = \omega_0 b_i^\dagger b_i + \frac{U}{2} (b_i^\dagger b_i)^2 \quad (3)$$

i.e. a characteristic frequency ω_0 and on-site Kerr non linearity of strength U while for the latter we consider two kinds ($\mu = 1, 2$) of jump operators for each lattice site i ,

$$L_{i2} = \sqrt{\eta} b_i b_i \quad (4)$$

$$L_{i1} = \sqrt{r} \sqrt{\eta} b_i^\dagger \quad (5)$$

describing respectively two-particles losses L_{i2} , with rate η , and single-particle incoherent pump L_{i1} , with rate ηr , where r is the pump-to-loss ratio. The resulting lattice model, Eq. (1-4), therefore describes a driven-dissipative realisation of the Bose-Hubbard model which is relevant both for Circuit QED arrays as well as for ultracold atoms in dissipative optical lattices. Its equilibrium properties are well understood in terms of a Mott-to-Superfluid transition [80] whose fate under drive and dissipation has been the subject of tremendous attention recently [32, 40, 53, 82–90] and will be one of the main focus of this work.

The many body master equation (2) has a global $U(1)$ symmetry, associated with the invariance of the Liouvillian with respect to the transformation $b_i \rightarrow b_i e^{i\theta}$, and is time translational invariant (TTI). The specific model (1-4) we consider is by itself rather unexplored, although few results are available in the literature that we will recall briefly here. In the limit of a large number of bosons per site one expects a semiclassical description to work. The model reduces then to a discretized

version of Gross-Pitaevskii equation, largely studied in the context of exciton-polariton condensation [36], which predicts a coherent phase of bosons for any $r > 0$, independently of J/U . This phase, which spontaneously breaks both the $U(1)$ and TTI symmetry corresponds to a nonequilibrium superfluid. In the opposite regime of uncoupled sites, $J/U = 0$, the steady-state density matrix is known analytically from [91, 92] and describes an incoherent state: it is a statistical mixture of Fock states with $\langle b_i \rangle = 0$, as might be expected given the lack of any coherent driving. How those two different phases are connected upon increasing J/U , in the quantum regime of few bosons per site and finite lattice connectivity is the main focus of this paper.

In Figure 2 we plot the Open-DMFT phase diagram as a function of r (the dimensionless drive-to-loss ratio) and J/U , for different values of the lattice connectivity z , together with the Gutzwiller mean field phase boundary corresponding to the $z = \infty$ limit [93]. For a given fixed value of z we find a critical line $r_c(J)$ separating a small-hopping normal phase where the bosons remain incoherent, $\langle b_i \rangle = 0$, from a large hopping phase where the system develops a local order parameter breaking the $U(1)$ symmetry of the master equation. A first striking result that clearly appears from Figure 2 is that upon decreasing the connectivity, i.e. increasing the strength of quantum fluctuations on top of the Gutzwiller mean field result, the phase diagram changes substantially. In particular the broken symmetry phase shrinks and moves toward larger values of drive. The shape of the phase boundary is also largely affected by finite connectivity corrections, much more than what one could have expected from the equilibrium case [66], in particular the re-entrant behavior of the normal phase found in mean-field disappears for small z . These are first signature of the importance of the correlations captured by Open-DMFT and our NCA impurity solver. Below we further elaborate on the origin of this effect and its physical interpretation, leaving to Sec. V for further details.

A transition in a Bose-Hubbard like model as a function of the hopping might look at first sight analogous to the equilibrium Mott to superfluid one. Instead, we show that both the properties of the normal phase and its instability are very different from their equilibrium counterparts and come with features which are unique to the driven-dissipative setting.

As we will discuss in more details in Sec. V A-V B, within the normal phase, two well separated crossover scales exist which signal a qualitative change in the spectral and distribution properties of the system. Above a drive threshold $r_{\text{ndos}} < r_c$ the system develops a negative density of states (NDOS) at positive frequencies, a genuine non-equilibrium effect which we show leads to energy emission in response to a weak coherent drive. Upon further increasing the drive above $r_{\text{ndos}} < r_{\text{inv}} < r_c$ the steady-state reduced density matrix shows population inversion, namely higher energy states become more occupied than lower energy ones. These two effects highlight

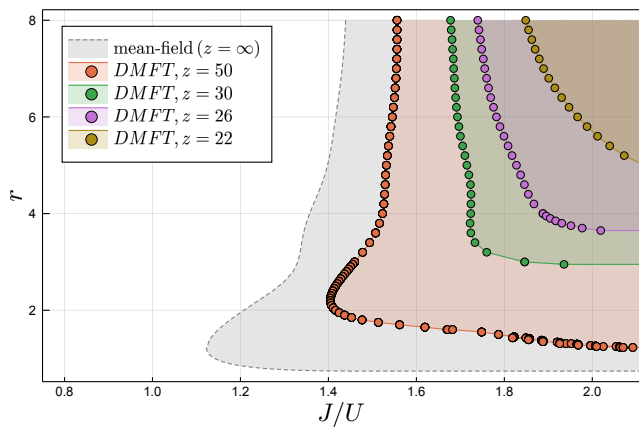


FIG. 2. Phase Diagram of the Bose-Hubbard model (see Eq.(1-4)) obtained with Open-DMFT and NCA, as a function of drive/loss ratio r and hopping/interaction ratio J/U , for different values of the lattice connectivity z , compared to the Gutzwiller mean-field one ($z = \infty$). A critical line $r_c(J)$ separates a normal low-hopping phase from a broken symmetry phase where the system develops a local order parameter oscillating in time at finite frequency. Decreasing the lattice connectivity, i.e. increasing quantum fluctuations due to the finite number of neighbors, the ordered phase shrinks and the entire phase boundary is reshaped. In particular the re-entrant behavior of the normal phase found in mean-field disappears at small values of z . Parameters: $\eta/U = 0.02$, $dt = 0.004$, $t_{max} = 10$, $dim_H = 10$ (see Sec. V).

the nonequilibrium nature of the stationary normal phase and strongly affect the instability toward $U(1)$ symmetry breaking at higher drives and the shape of the phase diagram at finite connectivity.

In Sec. VB we study the Open-DMFT predictions for the local steady-state populations. Open-DMFT includes hopping processes which are completely missed by mean-field theory. These are particularly interesting in open quantum systems, where they not only introduce coherent effects, but also open new dissipative channels: for example a particle can hop onto a neighbor site and get lost. Indeed, we show that these processes manifest in an overall reduction of steady-state on-site occupation and in a reduction of population inversion with increasing hopping.

In Sec. VC we show that an interplay of NDoS and sufficiently strong hopping J controls the true normal phase instability for drives above $r_c(J)$, when the system develops full phase coherence and enters the superfluid phase. In particular we find that the unstable mode is modulated in time and that the system displays a finite frequency phase transition corresponding to an order parameter which develops undamped oscillations, thus breaking TTI [90, 94, 95]. While this instability is present already at the level of Gutzwiller mean field theory (see $z = \infty$ results in Figure 1) quantum fluctuations captured by Open-DMFT lead to a quantitative reshape of

the phase boundary. Indeed we show that increasing the hopping J at fixed drive, both the two scales r_{ndos}, r_{inv} get strongly renormalized.

The driven-dissipative Bose-Hubbard (1-4) can be equivalently seen as a model for an array of quantum van der Pol (vdP) oscillators coupled by the hopping term J . In their classical formulation vdP oscillators represent textbook examples of non-linear dynamical systems [96–98]. In the quantum domain the one and few-body cases have been recently studied in the context of quantum synchronization [67–79]. As we show more in detail in Sec. VD, our model reduces in the semiclassical limit to an array of coupled classical vdP oscillators, which admits a stable limit cycle phase, a coherent phase with an order parameter oscillating in time at finite frequency, for any finite drive $r > 0$ and any coupling J . In the quantum regime of few bosons per site, the picture qualitatively changes and a transition arises as a function of hopping J depicted in Figure 2. This can be interpreted, in light of this analogy, as a quantum many body synchronization where above a certain coupling J all quantum VdP oscillators enter into a collective limit cycle phase.

The large reduction of the normal phase as z is decreased can be interpreted as a desynchronization effect due to quantum fluctuations encoded in the non-Markovian Open-DMFT bath. These fluctuations are able to wipe out the NDoS and absorb part of the energy emitted by the system as we discuss more in detail in Sec. VE. A complementary perspective to this reduction of the synchronized phase comes from the occupation properties of the normal phase. As we show in Sec. VE 3 the system develops an effective temperature, which for small drive values increases substantially upon decreasing the connectivity z , leading to heating and noise induced desynchronization.

We give a more complete picture of these results in Sec. V.

III. OPEN DYNAMICAL MEAN-FIELD THEORY

In this section we present the formalism of Open-DMFT, including the basic self-consistency equations, its formal relation with Gutzwiller mean field theory and its physical interpretation, leaving its derivation to Appendix A. The starting point is to cast the Lindblad master equation (2) in the language of non-equilibrium Keldysh field theory, as discussed extensively in the literature [51]. The result is an action written in terms of bosonic coherent fields $\bar{b}_{i\alpha}, b_{i\alpha}$ on each lattice site i and on the upper/lower Keldysh contours, $\alpha = \pm$, which takes the form

$$\mathcal{S} = \int_{-\infty}^{\infty} dt \sum_{i\alpha} \alpha \bar{b}_{i\alpha} i \partial_t b_{i\alpha} - \int_{-\infty}^{\infty} dt i \mathcal{L} \quad (6)$$

where the Lindbladian \mathcal{L} is given by

$$\mathcal{L} = -i(H_+ - H_-) + \sum_{\mu,i} \gamma_{\mu} \left(L_{i\mu+} \bar{L}_{i\mu-} - \frac{1}{2} \bar{L}_{i\mu+} L_{i\mu+} - \frac{1}{2} L_{i\mu-} \bar{L}_{i\mu-} \right) \quad (7)$$

with $H_{\alpha}, L_{i\mu\alpha}$ are the expectation values of the Hamiltonian (1) and of the jump operators (4), expressed in terms of creation and annihilation operators belonging to the α contour, taken on bosonic coherent states. The full solution of the Keldysh action in Eq.(6) is of course not possible in general, due to the coupling between many interacting modes and the presence of interaction, drive and dissipation.

The key idea of Open-DMFT is to write down an effective Keldysh action for the boson field of a single site of the lattice, obtained after integrating out all its neighbors [66]. As we show in Appendix A, in the limit of large lattice connectivity, $z \gg 1$, this effective action has the closed form

$$\mathcal{S}_{\text{eff}}[\mathbf{b}_{\alpha}^{\dagger}, \mathbf{b}_{\alpha}] = S_{\text{loc}}[\mathbf{b}_{\alpha}^{\dagger}, \mathbf{b}_{\alpha}] + \int dt \sum_{\alpha=\pm} \alpha \Phi_{\text{eff}\alpha}^{\dagger}(t) \mathbf{b}_{\alpha}(t) - \frac{1}{2} \int dt dt' \sum_{\alpha,\beta=\pm} \alpha \beta \mathbf{b}_{\alpha}^{\dagger}(t) \Delta^{\alpha\beta}(t, t') \mathbf{b}_{\beta}(t') \quad (8)$$

where we have dropped the site index from the local boson field for simplicity (we assume translational invariance) and grouped together creation/annihilation fields into a Nambu field

$$\mathbf{b}_{\alpha}^{\dagger} = \begin{pmatrix} \bar{b}_{\alpha} & b_{\alpha} \end{pmatrix} \quad \mathbf{b}_{\alpha} = \begin{pmatrix} b_{\alpha} \\ \bar{b}_{\alpha} \end{pmatrix} \quad (9)$$

The above local Keldysh action describes a driven-dissipative quantum impurity model [81]. The first term in Eq. (8), $S_{\text{loc}}[\mathbf{b}_{\alpha}^{\dagger}, \mathbf{b}_{\alpha}]$ is the local, on-site, contribution of the original lattice action (6-7) and therefore includes interactions, as well as Markovian drive and dissipation. The second and third terms describe the feedback of the rest of lattice onto the single site through its neighbors, in terms of an effective coherent drive $\Phi_{\text{eff}\alpha}^{\dagger}(t)$ and an effective non-Markovian bath with hybridization function $\Delta^{\alpha\beta}(t, t')$. Both these quantities have to be determined self-consistently, in particular the effective coherent drive reads

$$\Phi_{\text{eff}\alpha}^{\dagger} = J \Phi_{\alpha}^{\dagger}(t) + \int dt' \sum_{\beta=\pm} \beta \Phi_{\beta}^{\dagger}(t') \Delta^{\beta\alpha}(t', t) \quad (10)$$

and has two contributions, the first coming from the average of the bosonic field as in Gutzwiller mean field theory

$$\Phi_{\alpha}^{\dagger} = \langle \mathbf{b}_{\alpha}^{\dagger} \rangle_{S_{\text{eff}}} \quad (11)$$

and the second one coming from the non-Markovian bath, a non-trivial finite z correction accounting for the feedback of neighboring sites on the local effective field [66].

This latter term, whose origin will be discussed more in detail in Appendix A, plays a key role within Open-DMFT, in particular for what concerns the fluctuations corrections to phase diagram as we discuss in Sec. V C V E 2.

The self-consistency relation for the Green's function depends on the specific choice of the lattice. In the following we will use the simplified self-consistent relation for the Bethe lattice [66]

$$\Delta^{\alpha\beta}(t, t') = \frac{J^2}{z} \mathbf{G}^{\alpha\beta}(t, t') \quad (12)$$

where we have introduced the connected Green's function

$$\mathbf{G}^{\alpha\beta}(t, t') = -i \langle \mathbf{b}_{\alpha}(t) \mathbf{b}_{\beta}^{\dagger}(t') \rangle_{S_{\text{eff}}} + i \Phi_{\alpha}(t) \Phi_{\beta}^{\dagger}(t') \quad (13)$$

The Open-DMFT solution of the original Markovian lattice problem thus requires one to solve the Keldysh action (8), computing in particular the impurity Green's function (13) and the average of the bosonic field (11), for a given realization of the drive and the bath and to iterate (10-12) until self-consistency.

A. Limit of infinite coordination number: Gutzwiller Mean Field Theory

It is instructive at this point to take explicitly the limit of infinite coordination number $z \rightarrow \infty$. In this limit, the Open-DMFT effective action (14) becomes completely local in time

$$\mathcal{S}_{\text{eff}}[\mathbf{b}_{\alpha}^{\dagger}, \mathbf{b}_{\alpha}] \xrightarrow{z=\infty} S_{\text{loc}}[\mathbf{b}_{\alpha}^{\dagger}, \mathbf{b}_{\alpha}] + \int \sum_{\alpha} \alpha dt \Phi_{\text{eff}\alpha}^{\dagger}(t) \mathbf{b}_{\alpha}(t) \quad (14)$$

since the non-Markovian bath scales as $1/z$ (See Eq. 12), and as such can be unfolded back into a master equation for a single-site density matrix ρ , which satisfies

$$\partial_t \rho(t) = i[\mathbf{b}^{\dagger} \Phi(t), \rho] + \mathcal{L} \rho(t)$$

where \mathcal{L} is the local part of the Lindbladian and the feedback from the neighboring sites is carried by $\Phi(t) = \text{tr}[\mathbf{b} \rho(t)]$. This corresponds to a factorized Gutzwiller-like ansatz for the lattice many body density matrix

$$\rho_{\text{latt}}(t) = \prod_i \rho_i(t),$$

where i is the site index and $\rho_i(t) \equiv \rho(t)$ because of translational invariance. In other words we have explicitly shown that, as for equilibrium or closed systems [61, 66] also for driven-dissipative lattice systems the infinite connectivity limit of bosons coincides with Gutzwiller mean-field theory. We note that when $\Phi = 0$, this mean-field describes completely uncoupled sites, while Open-DMFT ($z < \infty$) captures the feedback from neighboring sites through the self-consistent bath Δ . In the following section we are going to add some physical intuition on how the Open-DMFT action (8) describes the effect of neighboring sites through a fictitious non-Markovian dissipation.

B. Open-DMFT Effective Action in the Classical/Quantum basis

We now give a physical interpretation to the various terms entering the Open-DMFT effective action in Eq. (8), in particular to the non-Markovian term. It is useful to introduce the so called classical and quantum components of the bosonic field

$$\mathbf{b}_{\text{cl/q}}(t) = \frac{\mathbf{b}_+ \pm \mathbf{b}_-}{\sqrt{2}} \quad (15)$$

$$\mathbf{b}_{\text{cl/q}}^\dagger(t) = \frac{\mathbf{b}_+^\dagger \pm \mathbf{b}_-^\dagger}{\sqrt{2}} \quad (16)$$

in terms of which we can re-write the Keldysh action as

$$\begin{aligned} \mathcal{S}_{\text{eff}} = & S_{\text{loc}}[\mathbf{b}_{\text{cl/q}}^\dagger, \mathbf{b}_{\text{cl/q}}] + \int dt \Phi_{\text{eff cl}}^\dagger \mathbf{b}_q + \\ & - \frac{1}{2} \int dtdt' (\mathbf{b}_q^\dagger(t) \Delta^R(t, t') \mathbf{b}_{\text{cl}}(t') + hc) + \\ & - \frac{1}{2} \int dtdt' \mathbf{b}_q^\dagger(t) \Delta^K(t, t') \mathbf{b}_q(t') \end{aligned} \quad (17)$$

In this basis only two independent combinations of the non-Markovian kernels $\Delta^{\alpha\beta}$ enter, namely the retarded component $\Delta^R(t, t') = \theta(t - t') (\Delta^{+-}(t, t') - \Delta^{-+}(t, t'))$, encoding the spectral properties of the bath and resulting in a frequency dependent damping for the bosonic mode which couples the classical and quantum components of the field, and the Keldysh component $\Delta^K = \Delta^{-+}(t, t') + \Delta^{+-}(t, t')$, encoding the occupation of the bath and resulting in a frequency dependent noise for the bosonic mode. It is worth stressing that the above Keldysh action contains quadratic, non-Markovian terms in the classical/quantum fields as well as non-linearities and higher powers of the classical/quantum fields included in the local part of the action $S_{\text{loc}}[\mathbf{b}_{\text{cl/q}}^\dagger, \mathbf{b}_{\text{cl/q}}]$. While the structure of Eq. (17) is a generic feature of Open-DMFT, the local part of the action depends on the particular form of local interaction and jump operators.

Finally, we can express also the impurity Green's functions Eq (13) in this basis to obtain the retarded Green's function and the Keldysh one

$$\mathbf{G}^R(t, t') = -i \langle \mathbf{b}_{\text{cl}}(t) \mathbf{b}_q^\dagger(t') \rangle_{S_{\text{eff}}} + i \Phi_{\text{cl}}(t) \Phi_q^\dagger(t') \quad (18)$$

$$\mathbf{G}^K(t, t') = -i \langle \mathbf{b}_{\text{cl}}(t) \mathbf{b}_{\text{cl}}^\dagger(t') \rangle_{S_{\text{eff}}} + i \Phi_{\text{cl}}(t) \Phi_{\text{cl}}^\dagger(t')$$

Those correlation functions contain crucial physical information about the local physics of the driven-dissipative lattice problem. The retarded Green's function in particular encodes information about the local excitation spectrum of the system and it is known to be a crucial probe for the transition from delocalization to Mottness in strongly correlated systems at equilibrium [59]. For open Markovian quantum systems the retarded Green's function contains, much like for closed equilibrium systems, information on the structure of the excitations on

top of the stationary state [99] and it directly probes dissipative phase transitions where those excitations become unstable. Its poles correspond to eigenvalues of the Lindbladian in the single particle sector, which come with a characteristic frequency and lifetime, and their (possibly complex) weight. The retarded Green's function has also a directly physical meaning: it describes the linear response of the expectation $\langle b(t) \rangle$ to a weak, classical field $h(t')$, which couples linearly to b^\dagger . In the case where b describes a photonic cavity mode, $G^R(t)$ can be directly measured by weakly coupling the cavity to an input-output waveguide and measuring the reflection of a weak probe tone (see e.g. [100, 101]).

The Keldysh Green's function on the other hand contains information about how the finite frequency excitations above the stationary state are populated. In thermal equilibrium those two functions are not independent, but constrained to satisfy the fluctuation-dissipation theorem [102].

C. Computing Lattice Quantities

Solving the Open-DMFT effective action and computing the impurity Green's functions (18) gives direct information on the local properties of the driven-dissipative lattice problem. Furthermore one can access non-local quantities, such as momentum distribution or non local correlation functions, through the lattice Green's functions at momentum \mathbf{k}

$$\mathbf{G}_{\mathbf{k}}^{\alpha\beta}(t, t') = -i \langle \mathbf{b}_{\mathbf{k}\alpha}(t) \mathbf{b}_{\mathbf{k}\beta}^\dagger(t') \rangle + i \Phi_{\mathbf{k}\alpha}(t) \Phi_{\mathbf{k}\beta}^\dagger(t'). \quad (19)$$

These satisfies a Dyson equation with a lattice self-energy $\Sigma^{\alpha\beta}(t, t')$, that within Open-DMFT is momentum independent [63, 64],

$$\mathbf{G}_{\mathbf{k}}^{\alpha\beta}(t, t') = \mathbf{g}_{\mathbf{k}}^{\alpha\beta}(t, t') + \sum_{\gamma\delta} \mathbf{g}_{\mathbf{k}}^{\alpha\gamma} \otimes \Sigma^{\gamma\delta} \otimes \mathbf{G}_{\mathbf{k}}^{\delta\beta}(t, t') \quad (20)$$

and coincides with the self-energy of the impurity problem

$$\mathbf{G}^{\alpha\beta}(t, t') = \mathbf{g}^{\alpha\beta}(t, t') + \sum_{\gamma\delta} \mathbf{g}^{\alpha\gamma} \otimes \Sigma^{\gamma\delta} \otimes \mathbf{G}^{\delta\beta}(t, t') \quad (21)$$

where in the above equations \otimes indicates time convolutions, $\mathbf{g}^{\alpha\beta}(t, t')$ are the Green's functions of the quantum impurity problem with no interactions, but including the non-Markovian bath Δ and $\mathbf{g}_{\mathbf{k}}^{\alpha\beta}(t, t')$ are the non-interacting lattice Green's functions.

IV. QUANTUM IMPURITY SOLVERS

In this section we present two methods to solve the quantum impurity model described by the Keldysh action (8) and compute in particular the impurity Green's functions, which are the key quantities in Open-DMFT.

We stress that this remains a challenging task due to the interactions on the impurity site (Kerr non-linearity and two-body losses in our case) and the non-Markovian nature of the bath. While no exact solution exists, different approaches have been proposed in recent years for DMFT in and out of equilibrium. The potentially most powerful techniques are based on diagrammatic Monte Carlo [103–108], giving numerically exact results, but in many cases these are affected by a severe sign-problem, limiting their applicability. In the non-equilibrium context, approximate solvers based on a resummation of non-crossing self-energy diagrams and its extensions, have been now extensively used [66, 109–114], together with other approaching extending exact diagonalization techniques [115].

A. Hubbard-I Approximation

The simplest approximation to solve the impurity problem (8) is based on perturbation theory in the non-Markovian bath kernel Δ , and its lowest order is known as the Hubbard-I approximation [59, 116]. As we will see this approach already gives a non-trivial hopping dependence of correlation functions which goes beyond Gutzwiller mean-field theory, but misses important correlations due to the non-Markovian bath. Our Open-DMFT approach will be based on the more powerful non-crossing approximation solver which we will introduce in the next section, but we will use Hubbard-I results for comparison and to motivate the need of a more powerful solver.

For simplicity, we formulate Hubbard-I in the normal phase, where $\Phi = 0$ and anomalous correlation functions vanish, thus we can restrict to the first Nambu component and refer to it with non-bold symbols, e.g. $G^{\alpha\beta} = \mathbf{G}_{11}^{\alpha\beta}$ where $\alpha, \beta = \pm$ are Keldysh indexes. We also focus on the stationary state regime, where Green's functions depend on time differences and we can move to the frequency domain i.e. $G^{\alpha\beta}(\omega)$, which is the case we will consider in our application in Sec. V.

The impurity Green's function obeys a Dyson equation, see Eq. (21), in terms of a self-energy $\Sigma^{\alpha\beta}(\omega)$ which contains the effect of interaction, drive and dissipation and which is in general a functional of the non-Markovian bath kernel $\Delta^{\alpha\beta}(\omega)$. Hubbard-I consists in approximating the impurity self-energy by its value for $\Delta = 0$, i.e. in absence of the bath, when it can be written as

$$\Sigma^{\alpha\beta}(\omega) \approx \left[g_0^{\alpha\beta}(\omega) \right]^{-1} - \left[G_0^{\alpha\beta}(\omega) \right]^{-1}. \quad (22)$$

Here $G_0^{\alpha\beta}(\omega)$ is the Green's function of the impurity site with interaction, drive and dissipation, but without the bath (the latter condition is indicated by the index 0); it can be computed numerically [99]. In contrast $g_0^{\alpha\beta}(\omega)$ corresponds to the Green's function of the impurity site in absence of the bath and without interactions (lower-case letter), which is known analytically. Plugging this self-energy back in the Dyson equation (21), and using

the self-consistency condition on the Bethe Lattice, we obtain a closed matrix equation for the Keldysh components of the local lattice Green's functions

$$\left[G^{\alpha\beta}(\omega) \right]^{-1} = \left[G_0^{\alpha\beta}(\omega) \right]^{-1} - \frac{J^2}{z} G^{\alpha\beta}(\omega) \quad (23)$$

The expressions of the retarded and Keldysh components are given explicitly in appendix D. In the appendix, we also show that the Hubbard-I approximation, despite introducing a beyond mean-field hopping dependence of Green's functions, still yields the same phase diagram as mean-field, motivating the need for a more powerful solver.

B. Non-Crossing Approximation

To go beyond the Hubbard-I approximation, we use the method developed in [81] which is particularly suited to solve Markovian quantum impurities coupled to a non-Markovian bath, as described by the action (8). We limit ourselves to sketching the derivation and giving key results, referring to [81] for more details. The idea is to perform a diagrammatic expansion in powers of Δ and to resum an infinite set of diagrams by solving a self-consistent Dyson-type equation. We remark that this expansion is carried out around an interacting problem, the single-site Markovian impurity, hence it is not based on Wick's theorem as in weak-coupling perturbation theories. As such, working directly with Green's functions is not convenient and the more natural formulation is in terms of evolution super-operators, that we will denote in the following with a hat. We start by defining the evolution super-operator $\hat{\mathcal{V}}$ of the reduced density matrix of the impurity

$$\rho_{\text{imp}}(t) = \hat{\mathcal{V}}(t, 0) \rho_{\text{imp}}(0) \quad (24)$$

formally obtained by tracing out the bath degrees of freedom. Since these are treated as non-interacting, only the single-particle Green's function of the bath enters the reduced dynamics, the kernel function Δ introduced in Eq. (8). Expanding this super-operator in powers of Δ we obtain a series which can be represented diagrammatically as shown in Fig. 3, where dashed lines represent the hybridization function Δ while solid lines represent the bare Markovian evolution super-operator $\hat{\mathcal{V}}_0(t, 0) = T \exp \left(\int_0^t dt' \hat{\mathcal{L}}_{\text{eff}}(t') \right)$, where T is the time-ordering and $\hat{\mathcal{L}}_{\text{eff}}(t) = \hat{\mathcal{L}}_0 + i[\hat{\mathbf{b}}^\dagger \Phi(t), \bullet]$ the effective single site Lindblad super-operator with argument \bullet .

This diagrammatic representation allows to define the self-energy \hat{S} of the series as the sum of one-particle-irreducible (1PI) diagrams, which cannot be cut into two disconnected parts by removing a solid line, and thus to formally resum the series into the Dyson equation

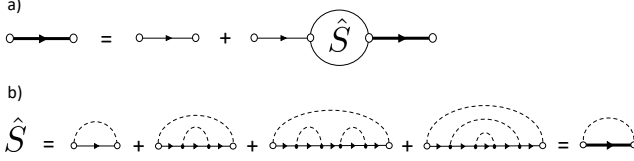


FIG. 3. a) Diagrammatic representation of the Dyson series in Eq. (25). The bold (thin) solid lines represent the full, non-Markovian (bare, Markovian) impurity super-operator $\hat{\mathcal{V}}$ ($\hat{\mathcal{V}}_0$), while the dashed lines correspond to the non-Markovian bath Δ . b) Expression of the self-energy \hat{S} in the NCA approximation, where only diagrams with non-crossing Δ lines are retained whose sum can be explicitly evaluated, see Eq. (26).

$$\hat{\mathcal{V}}(t, t') = \hat{\mathcal{V}}_0(t, t') + \int_{t'}^t dt_1 \int_{t'}^{t_1} dt_2 \hat{\mathcal{V}}_0(t, t_1) \hat{S}(t_1, t_2) \hat{\mathcal{V}}(t_2, t') \quad (25)$$

We remark that $\hat{\mathcal{V}}_0$, $\hat{\mathcal{V}}$ and \hat{S} here are super-operators and that the self-energy \hat{S} is a functional of the propagator $\hat{\mathcal{V}}$ whose closed form is not known in general. The resulting series (25) generalizes therefore to the case of Markovian impurities the hybridization expansion obtained for unitary quantum impurity models [104–106, 117, 118]. For the latter, exact resummation techniques based on diagrammatic Monte Carlo [103] have been employed but generically suffer from the so called sign problem, especially out of equilibrium, limiting the propagation time. Here instead we adopt a self-consistent approximation for the self-energy \hat{S} . This can be written in general as a systematic expansion in diagrams with an increasing number of crossing hybridization lines [109–112]. The lowest order contribution is given by non-crossing diagrams, e.g. in Fig. 3, giving an explicit expression for the NCA self-energy

$$\hat{S}(t_1, t_2) = -i \sum_{\substack{\alpha\beta \\ ab}} \alpha\beta \left[\Delta_{ba}^{\beta\alpha}(t_1, t_2) \hat{b}_{\beta b}^\dagger \hat{\mathcal{V}}(t_1, t_2) \hat{b}_{\alpha a} + \Delta_{ab}^{\alpha\beta}(t_2, t_1) \hat{b}_{\beta b} \hat{\mathcal{V}}(t_1, t_2) \hat{b}_{\alpha a}^\dagger \right] \quad (26)$$

In the above expression $\alpha, \beta = \pm$ are Keldysh indices and $a, b = \{1, 2\}$ are Nambu indices. Thus $\Delta_{ab}^{\alpha\beta}$ is a given component of the bath hybridization function introduced in Eq. (8), i.e. $\Delta_{ab}^{\alpha\beta} = (\Delta^{\alpha\beta})_{ab}$. We also introduce the super-operators analogues of the Nambu fields of Eq. (9), that we define as

$$\hat{\mathbf{b}}_\alpha^\dagger = (\hat{b}_\alpha^\dagger \hat{b}_\alpha) \quad \hat{\mathbf{b}}_\alpha = \begin{pmatrix} \hat{b}_\alpha \\ \hat{b}_\alpha^\dagger \end{pmatrix} \quad (27)$$

and denote their a Nambu component as $\hat{b}_{\alpha a}$ in Eq. (26). The Keldysh index $\alpha = \pm$ for a super-operator specifies whether it should act from the left or the right of its argument, i.e.

$$\hat{b}_+ = b \bullet \quad \hat{b}_- = \bullet b \quad (28)$$

and similarly for \hat{b}_α^\dagger . We notice that the self-energy depends on the full propagator $\hat{\mathcal{V}}$, rather than on the bare one $\hat{\mathcal{V}}_0$, thus containing diagrams to all orders in Δ . Corrections to the NCA can be obtained systematically including self-energy diagrams with higher number of crossings, although the resulting computational cost increases. In this work we will limit ourselves to the NCA scheme, since the experience obtained in the case of nonequilibrium DMFT for closed systems indicates that these corrections remain small within the normal (Mott) phase at strong coupling [111, 113, 114], which is the focus of

the present work. We also remark that the solver introduced in this section is different from standard NCA solvers for unitary quantum impurity models. Indeed its formulation at the level of evolution super-operators allows to fully capture the underlying local Markovian dynamics, resorting to an NCA approximation only for the non-Markovian, self-consistent environment introduced by Open-DMFT.

Once the self-energy \hat{S} is known in closed form, the propagator $\hat{\mathcal{V}}$ can be obtained numerically by solving Eqs. (25) and (26). To use this NCA impurity solver in our Open-DMFT approach, we need to compute the one-particle Green's functions of the impurity, Eq. (13), which are given by

$$G_{ab}^{\alpha\beta}(t, t') = -i \left\{ \text{tr} \left[\hat{b}_{\alpha a} \hat{\mathcal{V}}(t, t') \hat{b}_{\beta b}^\dagger \rho_{\text{imp}}(t') \right] \theta(t - t') + \text{tr} \left[\hat{b}_{\beta b}^\dagger \hat{\mathcal{V}}(t', t) \hat{b}_{\alpha a} \rho_{\text{imp}}(t) \right] \theta(t' - t) \right\} + i \Phi_{\alpha a}(t) \Phi_{\beta b}^\dagger(t') \quad (29)$$

where as before we have written explicitly both the Keldysh indices α, β and the Nambu ones a, b and where $\Phi_{\alpha a}(t) = \text{tr} [\hat{b}_{\alpha a} \rho_{\text{imp}}(t)]$. Eq. (29) can be derived by taking the functional derivative of the partition function $Z = \text{tr} [\rho_{\text{imp}}(\infty)] = \text{tr} [\hat{\mathcal{V}}(\infty, 0) \rho_{\text{imp}}(0)]$ with respect to

Δ and using the Dyson equation for $\hat{\mathcal{V}}$. We notice that this result, which resembles a quantum regression theorem for the non-Markovian map $\hat{\mathcal{V}}(t, t')$ is only valid within NCA, while including higher order diagrams into the self-energy would lead to further terms which can be interpreted as vertex corrections.

1. Stationary state Open-DMFT/NCA

In this section we show how to directly address the stationary state of the Dyson Equation (25) and the local Green's functions computed in this state, describing its time-dependent response and correlations, within our Open-DMFT/NCA approach. While the formalism introduced so far allows to compute the whole transient dynamics, focusing on the stationary state allows to significantly reduce the computational cost.

In this respect, we observe that once a stationary state is reached in the time evolution, the local Green's functions (13) depend only on time differences. This consideration allows to restrict the search for a self-consistent solution of the Open-DMFT equations (8-13) to Green's functions which only depend on time-differences. It also implies that all the quantities entering in the Dyson equation (25), namely the bath hybridization function $\Delta^{\alpha\beta}(t - t')$, the propagator $\hat{\mathcal{V}}(t - t')$ and self-energy $\hat{\mathcal{S}}(t - t')$ also depend on time differences, immediately reducing the numerical cost for time-propagating this equation from $O(t_{\max}^3)$ to $O(t_{\max}^2)$, where t_{\max} is the maximum integration time.

In order to evaluate the impurity Green's functions (29) entering in the Open-DMFT self-consistent equations, we first need to compute the stationary density matrix of the impurity $\rho_s \equiv \rho_{\text{imp}}(\infty)$, which also coincides with the on-site reduced density matrix of the original master equation (2). Assuming that such a density matrix exists, and that $\hat{\mathcal{L}}_{\text{eff}}(\infty)$ also exists, then it can be obtained by requiring the derivative of Eq. (25) to vanish at long times (see also [81] for the derivation), yielding the equation

$$\left(\hat{\mathcal{L}}_{\text{eff}}(\infty) + \int_0^\infty dt_1 \hat{\mathcal{S}}(t_1) \right) \rho_s = 0 \quad (30)$$

We observe that setting the NCA self-energy to zero, this equation reduces to well known condition for stationary states of Markovian master equations. In practice, to solve Open-DMFT/NCA for the stationary state, we solve the Dyson equation (25) for $\hat{\mathcal{V}}(t)$ starting from an initial ansatz for $\Delta(t - t')$, $\Phi(t')$ and ρ_s . As an initial condition we usually compute these quantities from the steady-state solution of the single-site problem. Then we compute the updated stationary density matrix ρ_s using Eq. (30) and the updated $\Delta(t - t')$, $\Phi(t')$ from Eqs. (10),(12) and iterate until convergence is reached.

V. OPEN-DMFT RESULTS FOR A DRIVEN-DISSIPATIVE BOSE-HUBBARD LATTICE

In this section we discuss our results for the driven-dissipative Bose-Hubbard model introduced in Sec. II B, comparing different impurity solvers (NCA and Hubbard-I approximation) and highlighting the effect of introducing quantum fluctuations beyond Gutzwiller mean-field due to the finite lattice connectivity. We start by discussing the properties of the normal phase at low hopping as encoded in its local spectral function (Sec. V A). We then move on to occupation properties of the nonequilibrium normal phase (Sec. V B) from the point of view of the local density and populations of the stationary-state reduced density matrix. In Sec. V C we discuss the dynamical, finite frequency, instability of the normal phase and the resulting non equilibrium phase transition, leading to the Open-DMFT phase diagram. We connect this instability to the physics of an array of quantum Van der Pol oscillators, in particular to the onset of many body synchronization and limit cycles (Sec. V D). Finally in Sec. V E we discuss the role of quantum fluctuations due to the finite connectivity z on the critical frequency and on the phase diagram comparing Open-DMFT with Gutzwiller mean-field theory.

Unless stated otherwise, we work in the regime where the interaction strength dominates the dissipation scale, i.e. we fix $\eta/U = 0.02$, and study the model as a functions of the drive/loss ratio r and the hopping to interaction ratio J/U . We put $\omega_0 = 1$, although we note that this scale only sets the zero of energy and can be eliminated by going to a rotating frame, so it does not play any role in the physics.

We introduce a cutoff on the local Hilbert space \dim_H , whose value will be specified for each result. We solve Open-DMFT for the normal phase, where $\Phi = 0$ and the anomalous (Nambu) Green's function components vanish so that the self-consistent bath only retains Keldysh indexes $\Delta^{\alpha\beta}$. The NCA propagator in the stationary regime $\mathcal{V}(t)$ is obtained, as described in Sec. IV B 1, by propagating in time the derivative of the Dyson equation (25) assuming time-translational invariance

$$\partial_t \hat{\mathcal{V}}(t) = \hat{\mathcal{L}}_0 \hat{\mathcal{V}}(t) + \int_0^t dt_1 \hat{\mathcal{S}}(t - t_1) \hat{\mathcal{V}}(t_1) \quad (31)$$

with an implicit second-order Runge-Kutta scheme [64], a propagation time $t_{\max} = 10$ and a time step $dt = 0.004$. We note that in the regime under consideration in this work the dynamics of the Dyson equation is dominated by the non-Markovian bath rather than by the two particle losses and therefore a $t_{\max} = 10 = 1/\eta$ is sufficient to reach convergence. Convergence of the implicit Runge-Kutta at each time step is assumed to be reached when $1/(\dim_H)^4 \sum_{jk} |\mathcal{V}_{jk}^{(i)}(t) - \mathcal{V}_{jk}^{(i-1)}(t)| < 10^{-5}$, being i the iteration index.

The convergence of the Open-DMFT scheme is assessed by checking that

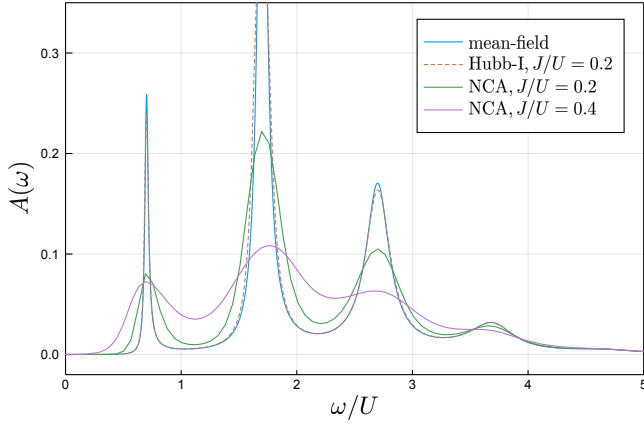


FIG. 4. Local spectral function $A(\omega)$ for different values of J/U , as computed within Gutzwiller mean-field theory (blue line), Open-DMFT with Hubbard-I impurity solver (dashed red line) and NCA impurity solver (green and violet line), for fixed $z = 6$ and $r = 0.6$. Gutzwiller results show a series of narrow peaks broadened by the local dissipation only. Open-DMFT instead is able to capture additional broadening processes, already evident for $J/U = 0.2$ within Hubbard-I, which however largely underestimates the effect of the non-Markovian bath as confirmed by the comparison with the more accurate NCA. Parameters: $\dim_H = 10$.

$1/(2t_{max}) \sum_{\alpha} \int_0^{t_{max}} |(\Delta^{\alpha, -\alpha})^{(i)}(t) - (\Delta^{\alpha, -\alpha})^{(i-1)}(t)| < 10^{-5}$, being i the index of the DMFT iteration. We have checked that our results essentially do not change by decreasing those thresholds or increasing the Hilbert space cutoff.

A. Spectral Function in the Normal Phase

To characterize the properties of the system, we first focus on the local retarded Green's function defined in Eq. (18). Since in the normal phase all anomalous (Nambu) Green's function components vanish as well as the average of the order parameter, we have only one independent Nambu component $G^R(t) = -i\theta(t)\langle[b(t), b^\dagger(0)]\rangle$. Its imaginary part defines the local spectral function

$$A(\omega) = -\frac{1}{\pi} \text{Im} G^R(\omega) \quad (32)$$

In Fig. 4 we plot the local spectral function in the low drive regime, $r = 0.6$, for different values of J/U and compare the Open-DMFT/NCA results with those obtained with Hubbard-I impurity solver and Gutzwiller mean-field.

A first important remark is that within Gutzwiller mean-field theory, corresponding to the infinite coordination number limit, the spectral function of the normal phase coincides with that of the single-site problem,

therefore losing all its dependence on the hopping J . Indeed in this limit, as we have discussed in Sec. III A, the only feedback from neighboring sites comes through the order parameter Φ , which vanishes in this phase. Including finite z corrections within Open-DMFT is therefore crucial to capture non trivial properties of the low hopping phase.

As we see in figure 4, the Gutzwiller mean-field spectral function shows a series of narrow peaks which are only broadened by the local dissipation. Open-DMFT instead is able to capture non-trivial correlations due coherent hopping processes, resulting in a further broadening of the resonances. This finite hopping correction to the spectral function reflects the fact that the stationary density matrix in the normal phase is *not* a tensor product of single-site density matrices, but rather includes correlations among neighboring sites, encoded within Open-DMFT in the non-Markovian bath. A comparison between Hubbard-I and NCA, shows that the former largely underestimates the effect of the bath. Indeed within NCA the sharp peaks of the isolated single site problem are largely broadened already for a moderate value of the hopping rate $J/U = 0.2$, a trend that further increases for larger values of J/U . At the same time the location of the poles is found to be weakly dependent on the hopping rate and, at least for $J/U = 0.2$, essentially captured already by Hubbard-I and Gutzwiller mean-field.

This difference can be understood by noticing that there are two main sources of resonance broadening within Open-DMFT, one coming from the bare non-Markovian bath $\Delta(\omega)$, the other coming from inelastic scattering encoded in the many body self-energy $\Sigma(\omega)$ (see Sec. III C). Within Hubbard-I (or Gutzwiller) the main contribution to $\Sigma(\omega)$ is real, giving rise to poles at frequencies of order U , with a small imaginary part coming from the weak Markovian dissipative processes which is subdominant to the bath contribution, roughly of order $\Delta \sim J^2/U$ for the frequency range in Figure 4. NCA on the other hand accounts for non trivial many body scattering channels mediated by the bath and results in a finite imaginary part of $\Sigma(\omega)$, also scaling with the hopping strength and responsible for the larger broadening. Overall the spectral function in this low-drive, low-hopping normal region is very reminiscent of an equilibrium Bose Hubbard model in the Mott insulating phase [116], with Hubbard bands, describing doublon/holons and multi-particle excitations, which are partially filled by drive and dissipation. As we show in the next section, increasing the drive strength reveals a spectral feature which is instead unique to interacting driven-dissipative systems.

1. Negative Density of States

We now discuss how the spectral features of the normal phase evolve upon increasing the strength of the drive/loss ratio r . While in the low drive regime all the

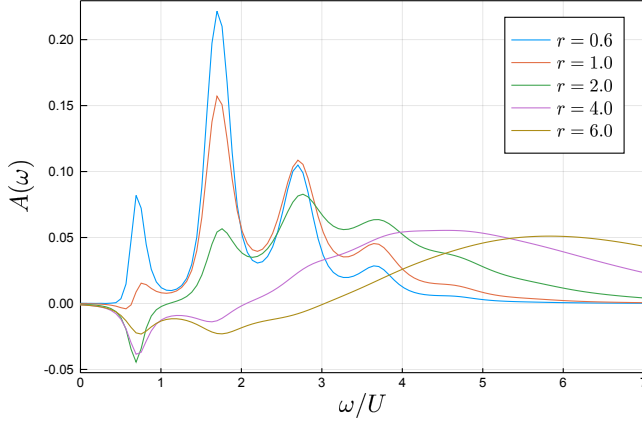


FIG. 5. Local spectral function $A(\omega)$ obtained from Open-DMFT/NCA for different values of the drive/loss ratio r at fixed $J/U = 0.2$ and $z = 6$. Upon increasing r the lowest Hubbard band flips sign and a region of Negative Density of States (NDoS) emerge at positive frequencies, up to $\omega = \Omega_0(r)$ where the spectral function vanishes, $A(\Omega_0) = 0$. The spectral range of NDoS increases with r . Parameters: $\dim_H = 14$.

peaks of the spectral function are positive, see Fig. 4, a novel effect appears at large drives. Above a threshold r_{ndos} the lowest Hubbard band flips sign and a region of *Negative Density of States* (NDoS) appears in a positive frequency range. We show this in Fig. 5 where we plot the spectral function obtained within NCA/DMFT for different values of drive/loss ratio r , at fixed $J/U = 0.2$. The region of NDoS extends up to $\omega = \Omega_0$, a frequency at which the imaginary part of the retarded Green's function linearly vanishes, i.e. we have

$$A(\omega) = \gamma(\omega - \Omega_0) \quad \text{for } \omega \simeq \Omega_0 \quad (33)$$

with $\gamma > 0$, while for $\omega > \Omega_0$ the conventional positive sign is recovered. As we show in figure 5 the spectral range of NDoS increases with the drive r and so does the frequency $\Omega_0(r)$. We stress that a negative spectral function at positive frequency is a genuine nonequilibrium phenomenon that cannot happen for closed systems in thermal equilibrium [99]. It has a direct physical consequences on the response of the system to a weak local coherent drive oscillating at frequency ω , $V(t) = \sum_i (v_i^*(t)b_i + \text{hc})$ with $v_i^*(t) = v_0\delta_{i,0}e^{i\omega t}$. Indeed for an open system the power absorbed from the perturbation, defined as [119–121] $\dot{W} = \text{Tr}\rho(t)\dot{V}$ can be written within linear response theory as (see appendix C)

$$\dot{W} = v_0^2\omega A(\omega) \quad (34)$$

This expression highlights how the spectral function at frequency ω controls the power absorbed by the system under an external drive. A change in sign of this quantity, i.e. a negative absorbed power, signals the onset of energy emission and gain, a condition which is generally associated to optical amplification and lasing [122–125].

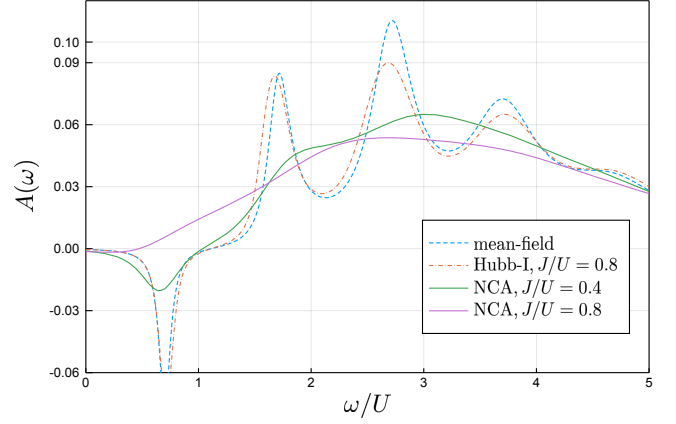


FIG. 6. Local spectral function $A(\omega)$ for different values of J/U , as computed within Gutzwiller mean-field theory (dashed blue line), Open-DMFT with Hubbard-I impurity solver (dashed pink line) and NCA impurity solver (green and red line), for fixed $z = 6$ and $r = 2$. Within the latter approach we see that increasing the hopping J changes qualitatively the structure of the low frequency spectrum, rectifying the NDoS and restoring a positive spectrum at $\omega > 0$. This effect of the Open-DMFT bath is completely missed by Gutzwiller mean-field as well as Hubbard-I approximations. Parameters: $\dim_H = 10$

As we are going to discuss in Sec V C the NDoS effect and the frequency Ω_0 will play a crucial role in the nonequilibrium phase transition from the normal to the superfluid phase.

We emphasize that the NDoS effect arises already in the single-site problem, i.e for $J = 0$ in our model, above a threshold drive r_{ndos} which depends on the strength of Kerr nonlinearity, as discussed in Ref. [99]. As a result, it naturally appears at large drive in the normal-phase spectral function of our lattice model calculated within Gutzwiller mean-field theory as well as DMFT/Hubbard-I, both built out of the exact solution of the single site problem.

An intriguing question is what happens to this NDoS region upon increasing the hopping strength between neighboring sites, while remaining well within the normal phase. Clearly such a question goes beyond Gutzwiller mean-field theory, which as we stressed cannot capture any non-trivial effects due to coherent hopping within the normal phase. In figure 6 we plot the spectral function obtained with DMFT/Hubbard-I and NCA, for increasing values of the hopping-to-interaction ratio J/U and compare with the results obtained from Gutzwiller. We find that, within NCA, the coupling to neighboring sites, i.e. the quantum fluctuations due to the finite connectivity of the lattice, strongly affects the spectral function at all frequencies, broadening the sharp high-energy peaks and decreasing the strength of the negative peak around Ω_0 , up to a value of $J/U \simeq 0.8$ at which this peak turns back to positive, washing away the NDoS effect. In other

words NCA is able to capture a non trivial renormalization of the scale Ω_0 from the coherent hopping J . Importantly, this effect is completely missed by the simple impurity solver Hubbard-I, whose spectral function, also shown in Figure 6, changes very little with respect to the Gutzwiller mean-field one. In fact one can show analytically, from the expression of the retarded Green function in appendix D, that Ω_0 in Hubbard-I is independent of the hopping and equivalent to the single-site and mean-field value. This result highlights the importance of including the feedback of the non-Markovian bath in the impurity self-energy, as done by summing up the infinite set of non-crossing diagrams.

To summarize, we have seen that changing drive and hopping largely affects the spectral properties of the normal phase. In particular we have identified for positive frequencies $0 < \omega < \Omega_0(r, J/U)$ a region of NDoS emerging above a threshold drive strength $r > r_{\text{ndos}}(J/U)$. Both these quantities depends non trivially from the hopping-to-interaction ratio J/U , an effect which is completely missed by Gutzwiller mean field as well as by Hubbard-I. As we are going to discuss in Sec. V C, these non-trivial dependencies of the critical frequency Ω_0 and of the threshold drive r_{ndos} from the hopping strength J , which are captured only by the NCA impurity solver, will have direct consequences on the phase diagram of the model.

B. Steady State Local Density Matrix and Population Inversion

We now discuss the occupation properties of the stationary state distribution in the normal phase. For a lattice problem computing the full many-body density matrix can be done only for very small systems. Nevertheless, within our Open-DMFT/NCA approach, describing the thermodynamic limit of infinitely-many sites, we can compute the reduced steady-state density matrix of a given site of the lattice, say site $i = 0$, obtained by performing a partial trace on all other sites, namely $\rho_s = \text{tr}_{j \neq 0} \rho_{\text{latt},s}$. This corresponds to the steady-state density matrix of the Open-DMFT self-consistent quantum impurity model (8) and thus of the non-Markovian map $\hat{\mathcal{V}}$ (24) and it obeys Eq. (30).

This reduced on-site stationary density matrix allows to study the change of the local populations of bosons due to hopping processes, which is completely inaccessible in Gutzwiller mean-field theory. Also, for open systems these hopping processes enable new, effective dissipative channels. For example a particle can be injected from the Markovian environment on one site, hop to another site and escape the system, rather than just being created and annihilated on the same site. Those processes are captured by our Open-DMFT approach and mimicked by the non-Markovian environment Δ and unlock interesting new physics which we are going to discuss here.

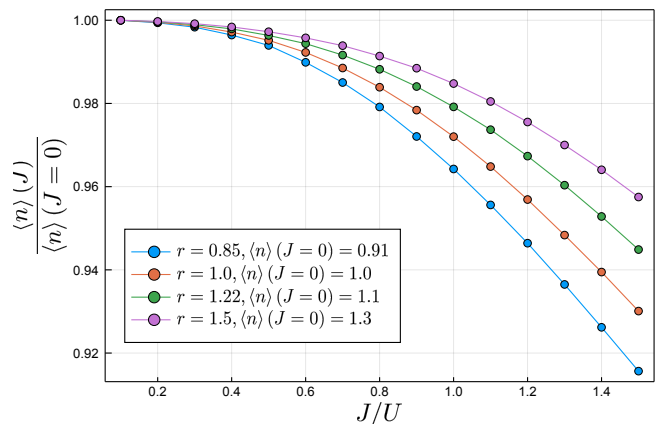


FIG. 7. Local density of particles as a function of the hopping to interaction ratio J/U , within Open-DMFT/NCA, for different values of the drive amplitude r , normalized to the values of the single site problem. We see that the density decreases with J/U , a specific feature of driven-dissipative lattices with two-body losses (see main text), which is captured by Open-DMFT. Parameters: $z = 50$, $\dim_H = 10$. The drive values used are marked on the y axis of Fig. 9.

1. Local Occupation vs J

From the knowledge of the on-site reduced stationary state density matrix ρ_s we can obtain the average local density $\langle n \rangle = \text{tr}(b^\dagger b \rho_s)$. We notice that the local density can be also obtained from the Green's functions, in particular from the Keldysh component at equal times

$$G^K(t, t) = -i \langle \{b(t), b^\dagger(t)\} \rangle = -i (2 \langle b^\dagger(t) b(t) \rangle + 1) \quad (35)$$

which gives consistently the same result in our NCA approach.

Within Open-DMFT the local density acquires a non trivial dependence from the hopping J , which is obviously missing in Gutzwiller mean field. In Fig. 7 we plot the density as a function of J/U at $z = 6$ and for different values of the drive, normalised to the mean-field value ($z = \infty$). We see that quite generically the density decreases smoothly upon increasing the hopping within the normal phase, i.e. for $J < J_c$. This can be understood as an interplay of two particle losses and coherent hopping between neighboring sites. This feature is mimicked within Open-DMFT by the bath $\Delta(\omega)$, which gives rise to effective single-particle non-Markovian losses for the bosons on the impurity site. This effect will be further explained by discussing the stationary-state populations in the next section. Interestingly the rate of decrease of the density with hopping changes quite strongly with the strength of the drive r and in particular we notice in Figure 7 that a large drive seems to make the density more pinned to the single-site value.

The result in Fig. 7 turns out to be a specific feature of dissipative lattices with two-particle losses. In fact

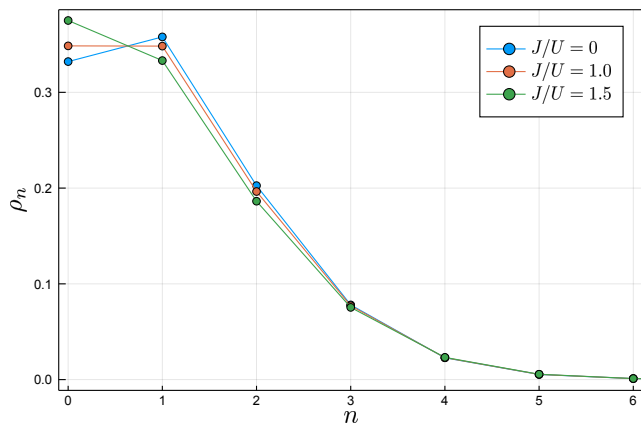


FIG. 8. Steady state populations of the reduced density matrix $\rho_n = \langle n | \rho_s | n \rangle$, within Open-DMFT/NCA, for different values of the hopping to interaction ratio J/U and for $r = 1.22$. We see that increasing J/U changes the populations at low values of n and ultimately washes away the population inversion found in the single site limit $J/U = 0$. Parameters: $z = 50$, $\dim_H = 10$. The drive value used are marked on the y axis of Fig. 9.

one can generically prove that for a driven-dissipative Bose-Hubbard model with only single particle losses and single particle drive the stationary state density matrix is independent of any Hamiltonian parameter [126], leading to a density of particles independent of J (although not necessarily integer, as it would be in the equilibrium Mott ground state of the Bose-Hubbard model) and only set by drive/loss balance. In App. B we show that this effect is correctly captured by our DMFT/NCA approach, a highly non-trivial benchmark for its validity.

2. Steady-State Populations and Population Inversion

In this section we discuss the effect of coherent hopping processes on the steady state reduced density matrix, which as we show exhibits richer physics than the local occupancy. In the normal phase this quantity is diagonal in the basis of Fock states with n bosons per site and the steady state populations ρ_n are shown in Fig. 8 for different hopping values, $z = 6$ and $r = 3$.

First we observe that the single-site model, corresponding to $J = 0$, shows a non-monotonic behavior of the populations as a function of the number of bosons per site, for drive/loss ratio $r > 1$ and any value of the Kerr non-linearity U (which in fact does not affect the stationary state as it has been long known [92]). This *population inversion* at $J = 0$ appears clearly in Fig. 8, where the probability of finding n bosons per site is maximum at $n = 1$ despite the fact that a finite bosonic occupation costs energy $E_n = \omega_0 n + U n^2 / 2 \sim U$ and should be therefore thermodynamically suppressed.

Increasing the hopping changes the populations at low

occupancy while leaving essentially unaffected the tail at large n . In particular, the coherent hopping from and into the neighboring sites increases the probability of having an empty site at expenses of finite occupation. This is a genuine feature of our dissipative many body lattice problem with local two body losses: starting from a state with average filling $n \sim 1$, hopping processes towards neighboring sites creates double occupations which escape at a rate η , reducing the total occupation. This trend goes on upon further increasing J , ultimately suppressing the population inversion above a threshold hopping. This mechanism also explains more in detail the observed overall decrease of average occupation with J , Fig. 7, which we already discussed in the previous section.

An interesting question concerns the relation between the NDoS effect discussed in Sec. V A and the population inversion in the reduced stationary density matrix. In closed quantum systems described by unitary evolution the two concepts are directly related, namely a NDoS could only emerge in presence of a inversion of populations where higher energy states are more occupied than lower energy ones. For open quantum systems the situation is more subtle and the two concepts are not in one-to-one correspondence [99]. In the next section we will discuss how those two effects evolve upon increasing the hopping and their impact on the instability of the normal phase towards a superfluid transition.

C. Finite Frequency Instability of the Normal Phase

In this section we discuss how the peculiar spectral and occupation properties of the normal phase contribute to an instability towards a spontaneous breaking of $U(1)$ symmetry. The key result is that the conventional static superfluid transition of the equilibrium Bose Hubbard model as a function of the hopping to interaction ratio is pushed to finite frequency as result of drive and dissipation, leading to an order parameter oscillating in time.

1. Open-DMFT Phase Boundary

Within our Open-DMFT approach, we can derive an equation for the phase boundary separating the normal and the broken symmetry phases. We assume to be in the early symmetry-broken phase, where the order parameter $\Phi(t) = \langle \mathbf{b}(t) \rangle$ has just formed and it is small. This implies a small external field $\Phi_{\text{eff}}(t)$ (10) in the Open-DMFT effective action (8). We also assume to be in a stationary regime at long times, such that two point correlators depend only on time differences, and move to Fourier space. The average value of the bosonic field $\Phi(\omega) \equiv \langle \mathbf{b}(\omega) \rangle$ is, to linear order in Φ_{eff}

$$\Phi(\omega) = -\mathbf{G}^R(\omega) \Phi_{\text{eff}}(\omega) \quad (36)$$

where we used the fact that $\langle \mathbf{b}(\omega) \rangle_{\Phi_{\text{eff}}=0} = 0$. A key point now is that at finite z the effective field $\Phi_{\text{eff}}(\omega)$ in Open-DMFT has two contributions, one from the local order parameter itself and the other from neighboring sites encoded in the non-Markovian bath, see Eq. (10) which now reads (using $\Phi_+ = \Phi_-$ as well as $\Phi_{\text{eff}+} = \Phi_{\text{eff}-}$)

$$\Phi_{\text{eff}}(\omega) = J\Phi(\omega) + \Delta^R(\omega)\Phi(\omega) \quad (37)$$

Plugging (37) into (36) and using the DMFT self-consistency on the Bethe lattice (12) one finally gets

$$\Phi(\omega) = \left(-J\mathbf{G}^R(\omega) - \frac{J^2}{z}\mathbf{G}^R(\omega)\mathbf{G}^R(\omega) \right) \Phi(\omega) \quad (38)$$

The critical coupling J_c and critical frequency Ω_c needed for a self-consistent broken-symmetry solution, $\Phi(\Omega_c) \neq 0$ corresponding to an order parameter oscillating in time $\langle b(t) \rangle \sim e^{-i\Omega_c t}$ for $J > J_c$, are given by

$$\frac{1}{J_c} + G^R(\Omega_c, J_c) + \frac{J_c}{z} [G^R(\Omega_c, J_c)]^2 = 0 \quad (39)$$

Equation (39), which to the best of our knowledge is an original result of this paper, is generic for bosonic DMFT theories on the Bethe lattice and it holds also for equilibrium problems. Its solution, leading to the phase boundary in Figures 2 and 9, strongly depends on the driven-dissipative nature of the problem, as we are going to discuss now. First, Eq. (39) has real and imaginary parts, which both need to vanish simultaneously, resulting in the two conditions

$$\text{Im}G^R(\Omega_c, J_c) = 0 \quad (40)$$

$$\frac{1}{J_c} + \text{Re}G^R(\Omega_c, J_c) + \frac{J_c}{z} [\text{Re}G^R(\Omega_c, J_c)]^2 = 0 \quad (41)$$

We remark that there is another solution possible, where $\text{Im}G^R(\Omega_c, J_c) \neq 0$, but this is never realized in our simulations. In thermal equilibrium the imaginary part of a retarded Green's function at positive frequency is in general different from zero except at $\omega = 0$, thus implying a static symmetry breaking pattern. Far from equilibrium this does not need to be the case [127] and indeed we have seen that the normal phase shows, above a threshold drive r_{ndos} , a spectral function vanishing at a positive frequency corresponding to the formation of a NDoS [90]. The critical frequency Ω_c solving Eq. (40) is therefore the point where the spectral function changes sign, while the critical hopping J_c is determined by jointly solving Eq. (41). We therefore conclude that the negative density of states discussed in previous section is a key, necessary condition for a phase transition into the superfluid phase.

This is clearly shown in Fig. 9, where we plot the threshold drive r_{ndos} for NDoS, discussed in the previous section, and the critical drive r_c obtained from solving Eq. (39) with Open-DMFT/NCA as a function of J/U . We see that generically $r_{\text{ndos}} < r_c$, namely the system

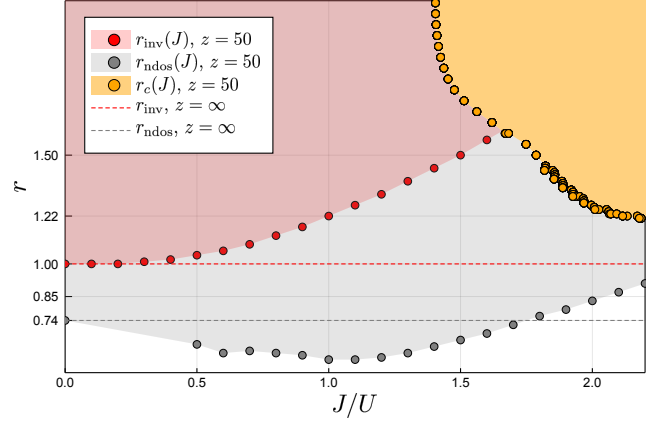


FIG. 9. Critical drive $r_c(J)$ (yellow points) for the finite-frequency superfluid transition as a function of the hopping, compared with the threshold drives for NDoS $r_{\text{ndos}}(J)$ and for population inversion in the density matrix $r_{\text{inv}}(J)$. The ticks of the y axis correspond to the values of r used for Figures 8 and 7. We see that for small value of r the phase transition occurs even in absence of a population inversion, i.e. it is the NDoS the key effect leading to the instability of the normal phase. Parameters: $z = 50$. Red curve: $t_{\text{max}} = 10$, $\text{dim}_H = 14$. Gray curve: $t_{\text{max}} = 20$, $\text{dim}_H = 10$.

first develops a NDoS and then becomes truly unstable towards $U(1)$ symmetry breaking. We will come back on this point in Sec. V E 2 when we will discuss the role of quantum fluctuations on the phase diagram.

A natural question is what is the role of the population inversion in the development of the normal phase instability. In Fig. 9 we compare the threshold drive/loss ratios for population inversion r_{inv} and for NDoS r_{ndos} , together with the phase boundary. We notice that those thresholds are independent from the hopping within Gutzwiller mean field (see dashed lines, which coincide with the $J = 0$ values of Open-DMFT) while they are substantially renormalized in Open-DMFT. In particular the two scales $r_{\text{ndos}} < r_{\text{inv}}$ further deviates from each other as the hopping is increased. As such we see, from the comparison with the phase diagram, that one can obtain an instability even in absence of population inversion.

We notice that the threshold for population inversion r_{inv} increases monotonically with the hopping strength J in Open-DMFT. Based on closed systems arguments, this *hopping-induced suppression* of population inversion would suggest that the NDoS is also always suppressed by hopping, as for example Fig. 6 shows. Surprisingly, this is not always the case. Figure 9 shows that r_{ndos} has a non-monotonic behavior with the hopping rate J , namely its behavior changes from small and large hopping values. While for large values of J the NDoS threshold r_{ndos} indeed increases following the behavior of the r_{inv} threshold, as expected from closed system arguments, for small values of J it is actually reduced below the $J = 0$ thresh-

old, corresponding to the single site. Namely, for small values of J , the non-Markovian bath Δ actually generates a NDoS, even in a regime where the single site model would not present any signature of this effect. This is a unique feature of dissipative quantum systems, where an NDoS can be generated even in absence of population inversion. For Markovian systems it has been showed that this can be traced back to the structure of excitations on top of the stationary state, which come with characteristic complex weights, leading to anti-lorentzian lineshapes [99].

We have focused so far on the critical coupling $r_c(J)$ for the phase transition and on the shape of the phase boundary obtained from Eq. (39), while we have not discussed yet the frequency Ω_c at which the system becomes unstable. As discussed in the previous section, this corresponds to the frequency at which the local spectral function of the normal phase vanishes, see Eq. (40), for the critical value of drive/loss ratio $r_c(J)$

$$\Omega_c = \Omega_0(r_c(J)) \quad (42)$$

In other words the energy scale Ω_0 appearing in the spectral function of the normal phase above threshold $r > r_{\text{ndos}}$ is a precursor of the mode that will become unstable at the transition. This scale appears in the spectral function, which as we mentioned could be measured in a transmission/reflection experiment for circuit QED arrays, and we expect it to emerge also in the normal phase dynamics approaching the stationary state in terms of coherent, yet damped, oscillations of the order parameter [90]. Showing those transient oscillations within Open-DMFT is possible, but goes beyond the scope of the stationary-state oriented approach (see Sec. IV B 1) used here.

D. Nonequilibrium Superfluidity, Limit Cycles and Many Body Synchronization of Van der Pol Arrays

The most striking result of previous section is the emergence of a spontaneous symmetry breaking at finite frequency. We now discuss how the nonequilibrium superfluid phase in this model can be equally interpreted as the onset of many body synchronization and limit cycles in an array of quantum Van der Pol oscillators [67–73]. To see this, it is convenient to write down the exact equation of motion for the average of the bosonic field at site i , $\partial_t \langle b_i \rangle = \text{Tr} \partial_t \rho b_i$, which reads using the Lindblad master equation (2)

$$\partial_t \langle b_i \rangle = -i\tilde{\omega}_0 \langle b_i \rangle - i\frac{\tilde{U}}{2} \langle n_i b_i \rangle - i\frac{U}{2} \langle b_i n_i \rangle + \frac{iJ}{z} \sum_j \langle b_j \rangle \quad (43)$$

where $\tilde{\omega}_0 = \omega_0 + i\frac{r\eta}{2}$, $\tilde{U} = U - 2i\eta$ and $n_i = b_i^\dagger b_i$. In the semiclassical limit, when the bosonic operator can be

replaced by a complex field $b_i \equiv \beta_i$, this reduces to

$$\partial_t \beta_i = -i \left(\omega_0 + i\frac{r\eta}{2} \right) \beta_i - i(U - i\eta) |\beta_i|^2 \beta_i + \frac{iJ}{z} \sum_j \beta_j \quad (44)$$

describing an array of coupled classical Van der Pol oscillators. In absence of any coherent drive the spatially uniform stationary state admits a stable limit cycle, i.e. $\beta(t) = |\beta| e^{-i\omega_{\text{vdp}} t}$ for any $r > 0$ with frequency ω_{vdp}

$$\omega_{\text{vdp}} = \omega_0 - J + U|\beta|^2 \quad (45)$$

and amplitude set by the drive, $|\beta| = \sqrt{r/2}$. Our driven-dissipative Bose-Hubbard model can be therefore also seen as a quantum many-body version of the VdP array. From this perspective, the onset of finite-frequency oscillations at $J_c(r)$ described in the last section can be seen as a signature of a quantum synchronized phase where above a certain coupling J all quantum VdP oscillators enter into a collective limit-cycle phase. As we are going to discuss next, these oscillations share qualitative features with the semiclassical solution at least at large drive values, while deviate significantly for smaller drives where quantum fluctuations are important. We emphasize however that the semiclassical approach cannot capture the transition into the normal, unsynchronized, phase whose properties we have extensively discussed in the previous sections. This requires a proper inclusion of quantum fluctuations, which is partially achieved by Gutzwiller mean field theory and more substantially by Open-DMFT as we are going to further elaborate on in Sec. V E.

1. Critical Frequency versus Drive/Loss Ratio and Kerr Non-Linearity

In this section we discuss the behavior of the critical frequency Ω_c , signaling the onset of a quantum synchronized phase, as a function of drive/loss ratio r and Kerr non-linearity U . In Figure 10 we plot this frequency as a function of the drive amplitude r , both for Open-DMFT (for $z = 50$) and for Gutzwiller mean field theory ($z = \infty$). We see that Ω_c scales linearly with the drive at large values of r (see fit in Fig. 10), a result which is in agreement with the semiclassical result obtained for the VdP array Eq. (45) where $\omega_{\text{vdp}}/U \sim r/2$. As the drive is reduced and the number of bosons per site decreases one expects quantum fluctuations to become more important. Indeed we see significant deviations from the semiclassical result at small r , already captured by Gutzwiller mean field but more pronounced for Open-DMFT.

Another interesting aspect is the role played by the Kerr non-linearity. In Fig. 11 we plot the local density of states for fixed value of hopping and drive/loss ratio and for different values of the interaction U . A first interesting observation is that the frequency Ω_0 at which NDoS emerges, related to the mode becoming critical at

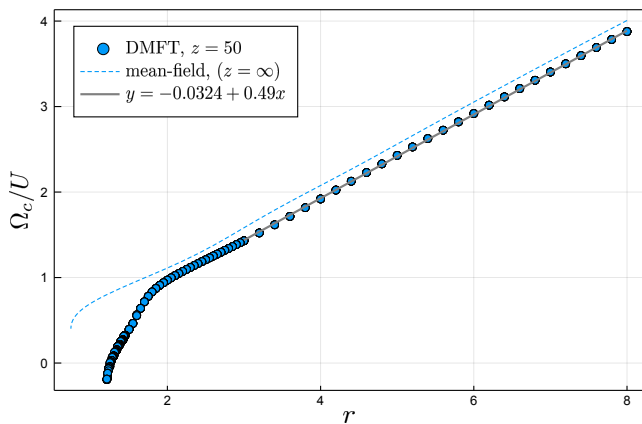


FIG. 10. Critical frequency for quantum synchronization Ω_c as a function of the drive/loss ratio r , within Open-DMFT/NCA for connectivity $z = 50$ and Gutzwiller mean field theory ($z = \infty$). In the region of large drive the fit shows that $\Omega_c/U \sim r/2$, in agreement with the semiclassical result for the limit cycle in the VdP array. At lower drives, in the regimes of few bosons per sites, quantum fluctuations become relevant and the critical frequency is strongly renormalized. Parameters: $\dim_H = 14$.

the synchronization transition (see Eq. (42), decreases upon reducing the Kerr non-linearity. A detailed analysis shows $\Omega_c \sim U$. We notice the analogy with the semiclassical result (45), nevertheless we stress that in this picture the critical frequency is proportional to the modulus square of the order parameter $|\langle b \rangle|^2 \neq 0$, while within Open-DMFT we find $\Omega_c \sim U$ at the critical point, where by definition $\langle b \rangle = 0$. This further highlights the quantum nature of the synchronization transition considered in this work. Indeed we have seen how Ω_c is smoothly connected to the frequency Ω_0 where NDoS emerges, a scale that exists already well inside the normal incoherent phase and that is a genuine feature of the quantum impurity model. Furthermore this implies that the Kerr non linearity is crucial in order to push the transition at finite frequency, implying undamped oscillations of the order parameter. We indeed observe that for a related model of all-to-all coupled quantum VdP oscillators [67] a recent Gutzwiller mean-field analysis reported a static (first-order) transition in absence of any Kerr non-linearity.

E. Role of Finite Connectivity

In this section we discuss in more detail the role of fluctuations induced by the finite lattice connectivity on the physics of the driven-dissipative Bose-Hubbard model, specifically their impact on the critical mode Ω_c going unstable at the transition and the critical drive/hopping as encoded in the phase diagram of the model. In particular we present two different perspectives on the reduc-

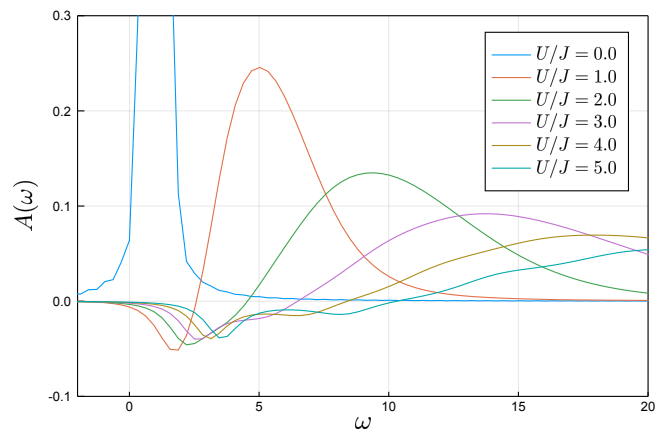


FIG. 11. Local spectral function $A(\omega)$ for increasing values of the Kerr non-linearity U , at fixed value of hopping $J = \omega_0$ and drive-to-loss ratio $r = 3$ within Open-DMFT/NCA. We see that the frequency Ω_0 at which the density of states vanishes, decreases with U and eventually disappears for small enough values of U . Parameters: $z = 6$, $\dim_H = 14$.

tion of the ordered phase observed in the Open-DMFT phase diagram (see Fig. 2). We highlight the role played by the non-Markovian self-consistent Open-DMFT bath which becomes more and more relevant as the connectivity is decreased from the Gutzwiller mean field theory at $z = \infty$ and the importance of treating this bath non-perturbatively as we do with our NCA approach.

1. Limit Cycles at Finite Connectivity

The existence of a limit cycle phase in a driven-dissipative quantum problem described by a time-independent Lindblad master equation is by itself non trivial. For finite-size systems, limit cycles can arise only in presence of dynamical symmetries [94] or decoherence free subspaces [128] and as such they do not correspond to extended phases, but they arise only in particular points of parameters space where those symmetries are enforced. In the thermodynamic limit of infinitely many degrees of freedom, instead, limit cycles can arise as collective phenomena in which particular modes of the system become dissipation-free. As such, limit-cycles can arise in an extended region of parameters space, namely constituting a non-equilibrium phase of matter, separated from other phases by phase transitions such as spontaneous symmetry breaking mechanisms. Limit-cycles emerge ubiquitously within mean field approaches [38, 129–131], and indeed even in the present problem the Gutzwiller solution at $z = \infty$ predicts one. The role of quantum fluctuations on their stability has been discussed before, in particular in the context of a coherently driven anisotropic Heisenberg model with spontaneous decay [132]. There an approach based on self-consistent Mori projection [133]

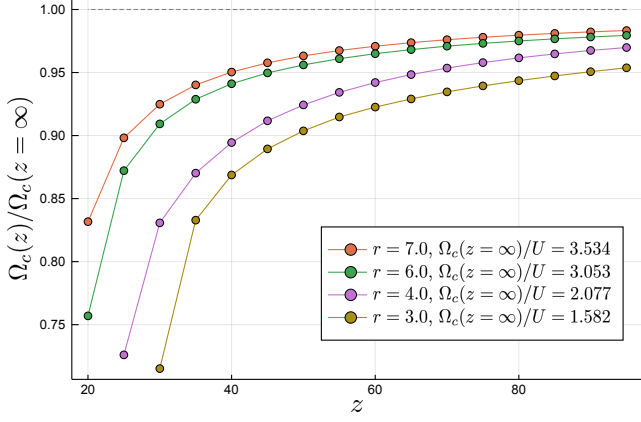


FIG. 12. Critical Frequency for quantum synchronization, Ω_c , within Open-DMFT/NCA, as a function of the lattice connectivity z , for different values of the drive-to-loss ratio r and hopping fixed on the phase boundary $J/U = (J/U)_c$. For clarity we normalize Ω_c to the mean field value obtained for $z = \infty$. We see that decreasing z renormalizes down the frequency, but does not destroy the limit cycle. Parameters: $\dim_H = 14$.

and cluster mean field [50] predicts that limit cycles disappear as the coordination number z is decreased below a threshold value z^* which depends on the system parameters.

On the basis of these results, it is particularly interesting to study the fate of our synchronization transition beyond Gutzwiller MFT theory. In Fig. 12 we plot the behavior of the critical frequency Ω_c obtained from Open-DMFT/NCA, as a function of z for different value of r . We observe that finite z corrections tend to reduce the value of Ω_c with respect to the mean field value, which nevertheless remains finite down to the lowest value of connectivity at which, for a given value of drive, a synchronization transition exists, consistently with the phase boundary moving to higher values of r for decreasing z (see Fig. 2). In other words we find that, within our treatment, finite connectivity does not destroy the limit cycle phase which is only pushed at higher values of the drive. Indeed in Fig. 12 we show that for drive $r = 7$, the highest value that we can numerically access given the constraints on the local Hilbert space truncation, a limit cycle would exist down to $z = 20$. We can therefore expect that this trend would continue even at higher drives and that the synchronized phase would survive down to low connectivity values. The regime of strong drive is however difficult to access within NCA and we leave this question open for future works. We remark nevertheless that our model is different from the one of Ref. [132]. In the present case the existence of a limit cycle phase is tightly related to a $U(1)$ symmetry present in the original Lindblad problem and spontaneously broken at the transition [90].

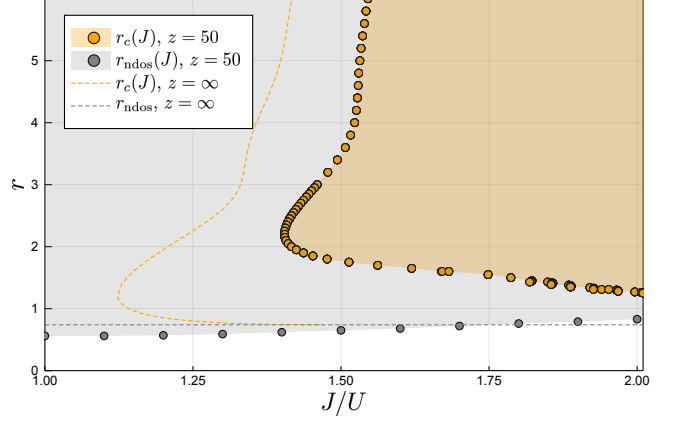


FIG. 13. Phase diagram in the drive/hopping plane obtained by Open-DMFT/NCA for $z = 50$ (yellow points) and Gutzwiller mean field theory ($z = \infty$, yellow dashed line). We further plots the thresholds for NDoS obtained within the two approaches. We see that quantum fluctuations due to finite connectivity reduces the broken symmetry phase (corresponding to nonequilibrium superfluidity/many body synchronization) pushing it towards higher values of hopping and drive. We interpret this effect as a desynchronization due to quantum and thermal fluctuations encoded in the Open-DMFT bath. Parameters: $\dim_H = 10$

2. Desynchronization from Quantum Fluctuations

We now compare the phase boundary in the drive versus hopping plane obtained with Open-DMFT/NCA and Gutzwiller mean field, see figure 2 and figure 13. We see that quantum fluctuations induced by a finite connectivity $z < \infty$ shift the phase boundary between normal and synchronized phase towards larger values of hopping J and drive/loss ratio r , substantially shrinking the synchronized phase. In other words, the quantum fluctuations included in Open-DMFT have a *de-synchronization* effect, delaying the onset of the many-body synchronization transition. We can understand this effect looking at Eq. (43) describing the quantum dynamics of the local bosonic operator. While at the semiclassical level, when bosons are fully coherent, the array of VdP oscillator would be always synchronized throughout the phase diagram, treating the bosons quantum mechanically introduce fluctuations in amplitude and phase which suppress the tendency towards symmetry breaking. Still, the way those fluctuations act on the system strongly depend on the value of lattice connectivity z , as it appears clearly by looking at the equation for the phase boundary (39). Within Gutzwiller mean field theory quantum mechanics enters only in the solution of the single site problem, while the feedback from neighboring site is treated still at a classical level, in terms of a self-consistent coherent field which reads $\Phi_{\text{eff}} = J\langle \mathbf{b}(t) \rangle \sim J e^{i\Omega_c t}$ near the instability. For $z \rightarrow \infty$ the equation for the phase boundary

reduces to

$$\frac{1}{J_c(z=\infty)} + G_0^R(\Omega_c) = 0 \quad (46)$$

where the first term is the effective field contribution and G_0^R is the retarded Green's function of the uncoupled single site. The latter develops a NDoS above a threshold drive (see gray dashed line in Figure 13) which is only controlled by the local drive/loss ratio r and does not depend on the hopping. The feedback from the neighboring sites, a classical coherent drive Φ_{eff} , acts as a seed for this almost unstable single mode. It triggers energy emission (negative absorbed power at Ω_c , see Eq. (34)) and leads above a threshold hopping to amplification of the local coherent field, a spontaneous symmetry breaking of $U(1)$ and time-translational symmetry resulting in a nonequilibrium superfluid, or a collective synchronized state of the quantum VdP oscillators.

Open-DMFT/NCA on the other hand accounts for a more subtle effect of neighboring sites, which are encoded through a frequency dependent quantum mechanical bath in addition to the classical coherent field. This has two important consequences. First, as already discussed, the non-Markovian bath is able to completely reshape the spectral features of the normal phase, wiping out for large enough hopping the NDoS region which we have shown to be a necessary condition for the onset of the instability. Second, a finite connectivity gives rise to a contribution order $\mathcal{O}(1/z)$ to the equation for the phase boundary, the last term in Eq. (39), which comes directly from the non-Markovian bath. As a result the Open-DMFT threshold for NDoS, controlling the onset of local gain, remains well separated from the critical drive responsible for the true many-body instability at intermediate coupling, as clearly seen in Figure (13), while approaching it at large hopping. The picture that emerges from Open-DMFT is therefore the one of a single quantum VdP oscillator on the verge of energy emission, coupled to an oscillating seed field which would favor optical amplification and embedded in a non-Markovian bath which is instead able to absorb part of the emitted power from the system, thus restoring absorption from gain and leaving behind a normal phase which would be synchronized otherwise. Quite interestingly this desynchronization from quantum fluctuations mechanism is not only completely missed by the Gutzwiller mean field approach, but also by a perturbative solver such as the Hubbard-I approximation. In fact we have discussed (see in figure 6) how the NDoS is changed very little within this scheme. In appendix D we also show that the Hubbard-I phase diagram, obtained using the non-trivial DMFT equation for the critical point (39), still reduces to the Gutzwiller mean-field one. This further highlights the non-perturbative nature of the quantum fluctuations responsible for the observed renormalization of the NDoS and the importance of using a self-consistent scheme such as our NCA approach.

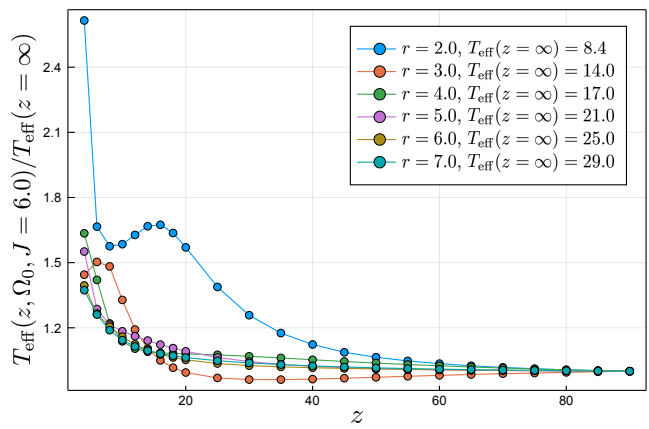


FIG. 14. Effective temperature T_{eff} obtained from the single particle distribution function (see main text) as a function of the lattice connectivity z , within Open-DMFT/NCA, for different values of the drive. We see that decreasing the connectivity leads to an increase of T_{eff} , particularly pronounced in the region of small drives. Parameters : $J/U = 1.2$, $t_{\text{max}} = 7.5$, $\text{dim}_H = 14$.

3. Fluctuations induced Heating

A different perspective on the role of quantum fluctuations at finite connectivity can be obtained by looking at the occupation of single particle modes at finite frequency, describing excitations on top of the stationary state and their effective thermal character. This physics is encoded in the Keldysh Green's function, defined in Eq (35), which heuristically describes the fluctuations of the observable b . If the system was in true thermal equilibrium, the quantum fluctuation-dissipation theorem (FDT) would constrain the Keldysh and the retarded components to obey the relation [102]

$$\frac{G^K(\omega)}{-2\pi i A(\omega)} \equiv F_{\text{eq}}(\omega) = \coth\left(\frac{\omega}{2T}\right) \quad (47)$$

where T is the system temperature. At low frequency or high temperatures, $\omega \ll T$, one has $F_{\text{eq}}(\omega) \sim T/\omega$. In a non-equilibrium system on the contrary there is no well-defined temperature and the FDT does not hold in general. Nonetheless, it is useful to use the left-hand side of the FDT relation in Eq. (47) to *define* an effective distribution function

$$F_{\text{neq}}(\omega) = \frac{iG^K(\omega)}{2\pi A(\omega)}$$

and to study its frequency dependence. Within the normal phase, for drive above the threshold for NDoS $r > r_{\text{ndos}}$, the spectral function $A(\omega)$ vanishes at frequency Ω_0 , with linear corrections (see Eq. (33)). On the other hand we find that the Keldysh component has a finite non-zero value at Ω_0 , which gives a distribution function of pseudo-equilibrium form at least for the modes

around Ω_0

$$F_{\text{neq}}(\omega) \simeq \frac{T_{\text{eff}}}{\omega - \Omega_0} \quad (48)$$

From this expression we can therefore identify an effective temperature T_{eff} , which emerges quite ubiquitously in nonequilibrium quantum systems [51, 134–138]. It is therefore particularly interesting to discuss the effective temperature of our system within the normal phase and the role of finite connectivity z . In figure 14 we plot the behavior of the effective temperature, at fixed $J/U = 1.2$ and scaled with respect to the mean field value, at $z = \infty$, as a function of the lattice connectivity z and for different values of the drive-to-loss ratio r . Notice that we have chosen a value of the hopping below the Gutzwiller mean field critical one, i.e. $J < J_c(z = \infty) < J_c(z)$, (see Figure 1), to make sure to always stay within the normal phase at any z .

At $z = \infty$, when Gutzwiller mean field is exact, the normal phase is described as a collection of independent sites. Yet an effective temperature emerges also in this limit of a single quantum VdP, due to the interplay of local drive and Kerr interaction [99]. Upon decreasing z we see that T_{eff} slightly increases, i.e. quantum fluctuations due to finite number of neighbors effectively heat up the system. As we see in Figure 14 this effect is particularly pronounced for small values of the drive to loss ratio, a regime where the destruction of the ordered phase in the phase diagram is most dramatic. This suggests a desynchronization phenomenon due to an effective noise [139, 140], encoded here in the non-Markovian bath. Open-DMFT provides a rather natural physical picture to understand this effect, especially on the Bethe Lattice. Indeed in this case the Keldysh Green's function of the impurity (35) directly maps into the Keldysh component of the non-Markovian bath $\Delta^K(\omega)$ through the self-consistency condition Eq.(12)

$$\Delta^K(\omega) = \frac{J^2}{z} G^K(\omega) \quad (49)$$

As a consequence the isolated single site (the mean field solution at $z = \infty$) becomes connected, at finite z , to a non-Markovian bath whose frequency modes around Ω_0 are effectively thermal at temperature T_{eff} . This provides further thermalisation channels to the system to convert the energy injection of the drive into heating and results in an increase of the effective temperature of the local impurity site. This result is particularly interesting in connection with the general phase diagram discussed in Figure 2 and provides further support to an effective thermalisation scenario for the reduction of the normal phase.

VI. CONCLUSIONS

Many experimental platforms for quantum simulations can be modeled as open-Markovian quantum lat-

tice problems where coherent Hamiltonian evolution coexists with local dissipative processes due to external environments. Their theoretical understanding poses new methodological and conceptual challenges which have stimulated a large activity in recent years.

In this paper we introduced a non-perturbative approach to bosonic systems described by a many body Lindblad master equation on lattice, based on a systematic expansion around the large lattice connectivity limit. This method can be seen as an extension of the dynamical mean field theory to open Markovian bosonic quantum systems. Within our Open-DMFT the local quantum fluctuations are treated non-perturbatively through the solution of a self-consistent quantum impurity model, where an interacting Markovian single-site problem is coupled to a coherent field and to a frequency dependent quantum bath mimicking the rest of the lattice. The non-Markovian frequency dependent bath contains the key new ingredient of Open-DMFT, which makes it different from other mean field approaches such as Gutzwiller mean-field theory, to which it reduces in the $z = \infty$ limit, or the semiclassical limit. In particular, with respect to the former, Open-DMFT is able to capture the physics of strongly correlated dissipative quantum phases which do not break any symmetry, such as bosonic Mott insulators and their dissipative counterparts.

Using Open-DMFT, together with a non-perturbative diagrammatic approach to solve the resulting impurity problem based on resummation of non-crossing diagrams in the impurity-bath coupling, we solved a Bose-Hubbard model in presence of two-particle losses and single particle pump, relevant for dissipative ultracold atoms. We unveiled the peculiar spectral and occupation properties of the model in its normal, incoherent phase, showing genuine nonequilibrium features such as NDoS and population inversion. We show that this normal phase becomes unstable at finite frequency, leading to a dynamical spontaneous breaking of the $U(1)$ and time-translation symmetry with an order parameter, the local bosonic field, coherently oscillating in time. Drawing from the physics of quantum VdP oscillators we interpreted this phenomenon as the onset of quantum many body synchronization and limit cycles. Finally we have discussed the role of finite lattice connectivity, the key feature of our Open-DMFT approach. We have shown that quantum fluctuations encoded in the Open-DMFT bath lead to a reduction of the ordered phase, a desynchronization effect that we interpreted further in terms of increased heating.

Our Open-DMFT holds the promise to be applied to a variety of driven-dissipative quantum many body problems. Different bosonic models or driving schemes can be considered and readily studied with the NCA approach developed here, such as the recently introduced quadratically driven Kerr resonator [40] or models relevant for the dissipatively stabilised Mott insulators of photons [16]. Interesting directions for the future involve the development of other quantum impurity solvers, by

mapping back the non-Markovian Keldysh action into a Lindbladian problem with a finite number of bath levels [65] which could then be solved by exact diagonalisation, quantum trajectories or through a matrix product operator representations of the density matrix, or the development of a cluster extension to Open-DMFT building upon recent developments [50]. Finally, we notice that a similar Open-DMFT construction as well as the NCA impurity solver, could be developed for driven-dissipative fermionic problems or quantum spins, which are also being actively investigated and relevant for different experimental platforms [141–145].

ACKNOWLEDGMENTS

This work was supported by the University of Chicago through a FACCTS grant (France and Chicago Collaborating in The Sciences), by the CNRS through the PICS-USA-147504, by a grant Investissements d'Avenir from LabEx PALM (ANR-10-LABX-0039-PALM) and from the ANR grant "NonEquMat" (ANR-19-CE47-0001). AC acknowledges support from the Air Force Office of Scientific Research MURI program, under Grant No. FA9550-19-1-0399.

Appendix A: Deriving DMFT for Open Markovian Quantum Systems

We present here a sketch of the derivation of the DMFT action and self-consistency conditions, using the quantum cavity method and following and extending Ref [66] to the open case. The main idea is to single out a given site of the lattice, $i = 0$ in the following, and to write down its effective Keldysh action obtained after integrating out all the other sites.

$$i\mathcal{S}_{\text{eff}}[\bar{b}_0, b_0] = \log \int \prod_{i \neq 0} D[\bar{b}_i, b_i] e^{i\mathcal{S}} \quad (\text{A1})$$

This effective single-site action describes, in principle, all the effects on site $i = 0$ due to the coupling to the other sites by the hopping J , which, for our assumption of local jump operators and interactions (Sec. II), is the only term responsible for the coupling between different sites. To proceed, we notice that the full action Eq. (6) can be divided in three terms,

$$\mathcal{S} = \mathcal{S}_0 + \delta\mathcal{S} + \mathcal{S}_{\text{cav}}^{(0)}$$

respectively $\mathcal{S}_0 = \mathcal{S}[\bar{b}_0, b_0]$ containing only the terms in Eqns. (6-7) involving fields at site $i = 0$, a term $\delta\mathcal{S}$ containing the hopping terms to the $2z$ fields (\bar{b}_j, b_j) at the neighboring sites

$$\delta\mathcal{S} = \frac{J}{z} \int dt \sum_{\alpha} \sum_{\langle 0j \rangle} (\bar{b}_{0\alpha} b_{j\alpha} + hc) \quad (\text{A2})$$

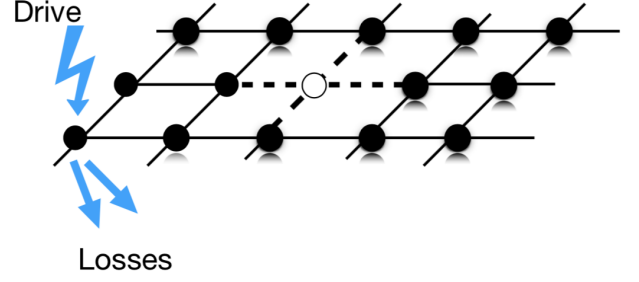


FIG. 15. Sketch of the quantum cavity method to derive the effective action of Open-DMFT for Markovian lattice problems (see text). A given lattice site is singled out (white dot in the figure) and all the remaining degrees of freedom are integrated out. Due to the coupling between the site and its $2z$ neighbors (dashed lines) this integration of degrees of freedom reduces to evaluate correlations function of a lattice with a cavity, containing all the remaining sites.

and a term $\mathcal{S}_{\text{cav}}^{(0)}$ describing a lattice with a cavity, namely including all the degrees of freedom except those at site $i = 0$, see Figure 15. For an interacting many-body problem on a finite dimensional lattice integrating over the neighboring sites can only be done formally, as a cumulant expansion in $\delta\mathcal{S}$, and leads to an effective action containing arbitrary powers of the local fields \bar{b}_0, b_0 , with coefficients given by the multipoints correlation functions of the cavity problem [59]. In the large connectivity limit, $z \gg 1$, one can formally organize this expansion in power of $1/z$ and obtain

$$\begin{aligned} \mathcal{S}_{\text{eff}}[\mathbf{b}_{0\alpha}^\dagger, \mathbf{b}_{0\alpha}] &= \mathcal{S}_0 + \int dt \sum_{\alpha=\pm} \alpha \Phi_{\text{eff}\alpha}^\dagger(t) \mathbf{b}_{0\alpha}(t) + \\ &+ \frac{i^2}{2} \int dt dt' \sum_{\alpha, \beta=\pm} \alpha\beta \mathbf{b}_{0\alpha}^\dagger(t) \Delta^{\alpha\beta}(t, t') \mathbf{b}_{0\beta}(t') \end{aligned} \quad (\text{A3})$$

where, in order to allow for condensed phases, we have introduced the Nambu-spinor notation

$$\mathbf{b}_0^\dagger = \begin{pmatrix} b_0 & \bar{b}_0 \end{pmatrix} \quad \mathbf{b}_0 = \begin{pmatrix} b_0 \\ \bar{b}_0 \end{pmatrix}$$

The coefficients entering the effective action (A3) are related to quantum averages over the cavity action $\mathcal{S}_{\text{cav}}^{(0)}$

$$\Phi_{\text{eff}\alpha}^\dagger(t) = J/z \sum_{\langle j0 \rangle} \langle \mathbf{b}_{j\alpha}^\dagger(t) \rangle_{\text{cav}}^{(0)} \quad (\text{A4})$$

$$\Delta^{\alpha\beta}(t, t') = J^2/z^2 \sum_{\langle j0 \rangle \langle k0 \rangle} \langle \mathbf{b}_{k\alpha}(t) \mathbf{b}_{j\beta}^\dagger(t') \rangle_{\text{cav}}^{(0)} \quad (\text{A5})$$

The final step, in order to obtain the self-consistent conditions, is to relate the average of bosonic fields on the cavity action to those evaluated to the effective action (A3). For what concerns the non-Markovian bath in Eq. (A5) this depends on the lattice geometry: it

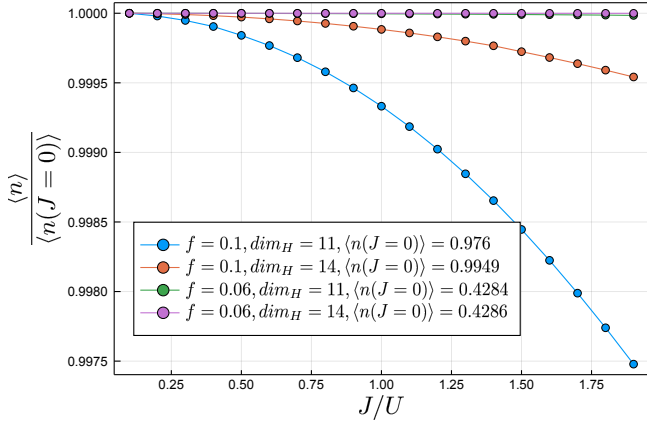


FIG. 16. Local density of particles for the BH model with single-particle losses, as a function of the hopping to interaction ratio J/U , for different values of the drive amplitude f , normalized to the values of the single site problem. Parameters: $z = 30$, $\kappa = 0.2$, $dt = 0.005$.

becomes particularly transparent for a Bethe lattice, a lattice with no loops such that once a cavity is created two neighbors j, k are completely disconnected, where one gets

$$\begin{aligned} \langle \mathbf{b}_{k\alpha}(t) \mathbf{b}_{j\beta}^\dagger(t') \rangle_{cav}^{(0)} &= \delta_{kj} \langle \mathbf{b}_{j\alpha}(t) \mathbf{b}_{k\beta}^\dagger(t') \rangle_{cav}^{(0)} = \\ &= \delta_{kj} \langle \mathbf{b}_{j\alpha}(t) \mathbf{b}_{j\beta}^\dagger(t') \rangle_S = \delta_{kj} \langle \mathbf{b}_{0\alpha}(t) \mathbf{b}_{0\beta}^\dagger(t') \rangle_{S_{\text{eff}}} \end{aligned} \quad (\text{A6})$$

where we have used the property of the Bethe lattice in the first equality, the fact that in thermodynamic limit the local property of the cavity action and the original action must be the same in the second equality and translational invariance in the last step. Plugging this into Eq. (A5) gives the self-consistency condition (12). We notice that similar arguments can be used for a different lattice, to relate averages over cavity and effective action, the only difference would be a more complicated self-consistency relation between bath and local Green's function [59]. Finally, the average of the bosonic field taken on the cavity action can be related to the one on the effective action (A3) as [66]

$$\begin{aligned} \langle \mathbf{b}_{j\alpha}^\dagger \rangle_{cav}^{(0)} &= \langle \mathbf{b}_{0\alpha}^\dagger \rangle_{S_{\text{eff}}} + \\ \int dt' \sum_{\beta=\pm} \beta \langle \mathbf{b}_{0\beta}^\dagger(t') \rangle_{S_{\text{eff}}} \langle \mathbf{b}_{k\beta}(t) \mathbf{b}_{j\alpha}^\dagger(t) \rangle_{cav}^{(0)} \end{aligned} \quad (\text{A7})$$

which can be plugged in Eq. (A4) to give the second self-consistent condition (10).

Appendix B: Benchmark: Local Occupation with Single-Particle Losses

In this appendix we report a non-trivial benchmark our Open-DMFT/NCA approach for driven-dissipative

many-body master equations defined by Eqs. (2) and (1). We consider a different model from the main text, namely the driven-dissipative Bose-Hubbard model with single-particle losses and single-particle drive. This is specified by the same Bose-Hubbard Hamiltonian Eqs. (1) and (3) as in the main text, but with the jump operators

$$\hat{L}_{i,l} = \sqrt{\kappa} \hat{b}_i \quad (\text{B1})$$

$$\hat{L}_{i,p} = \sqrt{f} \hat{b}_i^\dagger \quad (\text{B2})$$

where there is single-particle losses instead of the two-particle losses of the main text.

One can prove [126] that the stationary state density matrix of this model is independent from any Hamiltonian parameter, thus, for example, the on-site occupation is constant with the hopping rate J is a highly non-trivial benchmark for our Open-DMFT/NCA approach. Figure 16 shows that this behavior is correctly reproduced by our approach. Small deviations from constant occupation show that this property is not exactly enforced by our numerical scheme and thus is a good test to validate our approach. Deviations from constant occupation are mostly a result of local Hilbert space truncation, which become more severe increasing the drive, but they are reduced by increasing the cutoff \dim_H .

Appendix C: NDoS and Response to a Weak Coherent Drive

In this appendix we show that a direct consequence of the NDoS effect is that the average power absorbed from a weak coherent drive becomes negative, indicating the onset of gain and energy emission. We consider our lattice model in presence of a time dependent perturbation of the Hamiltonian describing a weak coherent drive with frequency ω

$$H(t) = H + V(t) \equiv H + \sum_i \left(v_i^* e^{i\omega t} b_i + v_i e^{-i\omega t} b_i^\dagger \right) \quad (\text{C1})$$

where H is the Bose Hubbard Hamiltonian defined in Eq.(1-3). The evolution of the density matrix of the system is described by the Lindblad master equation in presence of $H(t)$

$$\partial_t \hat{\rho} = -i[H(t), \hat{\rho}] + \sum_{i\mu} \left(\hat{L}_{i\mu} \hat{\rho} \hat{L}_{i\mu}^\dagger - \frac{1}{2} \{ \hat{L}_{i\mu}^\dagger \hat{L}_{i\mu}, \hat{\rho} \} \right) \quad (\text{C2})$$

We notice that the time derivative of the internal energy $E(t) = \langle H(t) \rangle$ in an open quantum system has two contributions, respectively coming from the derivative of the system Hamiltonian and from the time derivative of the density matrix

$$\dot{E}(t) = \text{Tr}(\dot{\rho}(t) H(t)) + \text{Tr}(\rho(t) \dot{H}(t)) \quad (\text{C3})$$

the latter being identified as heat flow which would be zero in a closed system evolving with unitary dynamics.

We are interested in the first term which measures the absorbed power from the external perturbation [121] and can be written as

$$\dot{W}(t) = \text{Tr} \rho(t) \dot{H}(t) = \sum_i (i\omega v_i^* e^{i\omega t} \langle b_i \rangle + \text{hc}) \quad (\text{C4})$$

Within linear response theory the average of the bosonic field can be written as

$$\langle b_i \rangle = \sum_j \int dt' G_{ij}^R(t-t') v_j(t') \quad (\text{C5})$$

where $G_{ij}^R(t-t') = -i\theta(t-t') \langle [b_i(t), b_j^\dagger(t')] \rangle$. Plugging this expression into Eq. (C4) we obtain the average absorbed power

$$\dot{W} = \sum_{ij} v_i^* v_j \omega A_{ij}(\omega) \quad (\text{C6})$$

written in terms of the spectral function $A_{ij}(\omega) = (-1/\pi) \text{Im} G_{ij}^R(\omega)$. For a localized perturbation, $v_i = v_0 \delta_{i,0}$ we obtain the result given in the main text, showing how a NDoS implies a negative absorption rate, namely the system transfer some of the energy from the perturbation to the emitted radiation.

Appendix D: Hubbard-I Impurity Solver

In this appendix we compute the impurity Green's functions in the simple Hubbard-I approximation discussed in Sec. IV A and show that the phase diagram computed in Hubbard-I coincides with the mean-field one. We restrict to study the symmetric phase, i.e. $\Phi = 0$, where equations involve one Nambu component and to the stationary regime where convolutions turn into product under Fourier transform.

Equation (23) is a closed second-order algebraic equation for $G^{\alpha\beta}(\omega)$, which is easily solved in the classi-

cal/quantum basis for the retarded and Keldysh components. The retarded Green's function is simply given by taking its retarded component, yielding

$$J^2/z G^R(\omega) = [G_0^R(\omega)]^{-1} - [G^R(\omega)]^{-1} \quad (\text{D1})$$

which can be solved and gives

$$G^R(\omega) = \frac{z}{2J^2} G_0^R(\omega)^{-1} \left(1 - \sqrt{1 - \frac{4J^2}{z} G_0^R(\omega)^2} \right) \quad (\text{D2})$$

The inverse Keldysh Green's function is given by $[G^{-1}]^K = [G_0^{-1}]^K - \frac{J^2}{z} G^K$, that we invert with the standard relation $G^K = -G^R [G^{-1}]^K G^A$ giving

$$G^K(\omega) = \frac{|G^R(\omega)|^2 G_0^K(\omega)}{|G_0^R(\omega)|^2 \left(1 - \frac{J^2}{z} |G^R(\omega)|^2 \right)} \quad (\text{D3})$$

We finally show that the Hubbard-I impurity solver gives the same phase boundary and critical frequency as Gutzwiller mean-field. In fact if we plug the equation for the Hubbard-I retarded Green's function, Eq. (D1), into the equation for the finite-frequency transition in DMFT, Eq. (39) that we rewrite for convenience here

$$\frac{1}{J_c} + G^R(\Omega_c, J_c) + \frac{J_c}{z} [G^R(\Omega_c, J_c)]^2 = 0 \quad (\text{D4})$$

we obtain

$$G^R(\Omega_c, J_c) \left(J_c + [G_0^R(\Omega_c)]^{-1} \right) = 0 \quad (\text{D5})$$

where the term in parenthesis is exactly the Gutzwiller mean-field condition for critical hopping and frequency (see Eq. (46) or Eq. (39) for $z = \infty$). We conclude therefore that the reduction of the ordered phase discussed in the main text and the dependence of Ω_c from the hopping are key features of the NCA impurity solver.

-
- [1] J. I. Cirac and P. Zoller, “Quantum computations with cold trapped ions,” *Phys. Rev. Lett.* **74**, 4091–4094 (1995).
 - [2] J. M. Raimond, M. Brune, and S. Haroche, “Manipulating quantum entanglement with atoms and photons in a cavity,” *Rev. Mod. Phys.* **73**, 565–582 (2001).
 - [3] R. J. Schoelkopf and S. M. Girvin, “Wiring up quantum systems,” *Nature* **451**, 664–669 (2008).
 - [4] Markus Aspelmeyer, Tobias J. Kippenberg, and Florian Marquardt, “Cavity optomechanics,” *Reviews of Modern Physics* **86**, 1391–1452 (2014).
 - [5] Immanuel Bloch, Jean Dalibard, and Sylvain Nascimbène, “Quantum simulations with ultracold quantum gases,” *Nature Physics* **8**, 267 EP – (2012).
 - [6] Antoine Browaeys and Thierry Lahaye, “Many-body physics with individually controlled rydberg atoms,” *Nature Physics* **16**, 132–142 (2020).
 - [7] R. Blatt and C. F. Roos, “Quantum simulations with trapped ions,” *Nature Physics* **8**, 277 EP – (2012).
 - [8] Andrew A. Houck, Hakan E. Türeci, and Jens Koch, “On-chip quantum simulation with superconducting circuits,” *Nature Physics* **8**, 292–299 (2012).
 - [9] Y. Salathé, M. Mondal, M. Oppliger, J. Heinsoo, P. Kurpiers, A. Potočnik, A. Mezzacapo, U. Las Heras, L. Lamata, E. Solano, S. Filipp, and A. Wallraff, “Digital quantum simulation of spin models with circuit quantum electrodynamics,” *Physical Review X* **5**, 21027 (2015).
 - [10] Javier Puertas Martínez, Sébastien Léger, Nicolas Gheeraert, Rémy Dassonneville, Luca Planat, Farshad Foroughi, Yuriy Krupko, Olivier Buisson, Cécile Naud, Wiebke Hasch-Guichard, Serge Florens, Izak Snymman,

- and Nicolas Roch, “A tunable Josephson platform to explore many-body quantum optics in circuit-QED,” *npj Quantum Information* **5**, 19 (2019).
- [11] Iacopo Carusotto, Andrew A. Houck, Alicia J. Kollár, Pedram Roushan, David I. Schuster, and Jonathan Simon, “Photonic materials in circuit quantum electrodynamics,” *Nature Physics* **16**, 268–279 (2020).
 - [12] J. M. Fink, A. Dombi, A. Vukics, A. Wallraff, and P. Domokos, “Observation of the Photon-Blockade Breakdown Phase Transition,” *Phys. Rev. X* **7**, 11012 (2017).
 - [13] Mattias Fitzpatrick, Neereja M. Sundaresan, Andy C.Y. Y Li, Jens Koch, and Andrew A. Houck, “Observation of a Dissipative Phase Transition in a One-Dimensional Circuit QED Lattice,” *Phys. Rev. X* **7**, 11016 (2017).
 - [14] Thomas Fink, Anne Schade, Sven Höfling, Christian Schneider, and Ataç Imamoglu, “Signatures of a dissipative phase transition in photon correlation measurements,” *Nature Physics* **14**, 365–369 (2018).
 - [15] J. Raftery, D. Sadri, S. Schmidt, H. E. Türeci, A. A. Houck, H. E. Türeci, and A. A. Houck, “Observation of a dissipation-induced classical to quantum transition,” *Physical Review X* **4**, 031043 (2014).
 - [16] Ruichao Ma, Brendan Saxberg, Clai Owens, Nelson Leung, Yao Lu, Jonathan Simon, and David I. Schuster, “A dissipatively stabilized Mott insulator of photons,” *Nature* **566**, 51–57 (2019).
 - [17] N. Syassen, D. M. Bauer, M. Lettner, T. Volz, D. Dietze, J. J. García-Ripoll, J. I. Cirac, G. Rempe, and S. Dürr, “Strong dissipation inhibits losses and induces correlations in cold molecular gases,” *Science* **320**, 1329–1331 (2008), <https://science.sciencemag.org/content/320/5881/1329.full.pdf>
 - [18] Takafumi Tomita, Shuta Nakajima, Ippei Danshita, Yosuke Takasu, and Yoshiro Takahashi, “Observation of the mott insulator to superfluid crossover of a driven-dissipative bose-hubbard system,” *Science Advances* **3** (2017), 10.1126/sciadv.1701513.
 - [19] Henrik P. Lüschen, Pranjal Bordia, Sean S. Hodgman, Michael Schreiber, Saubhik Sarkar, Andrew J. Daley, Mark H. Fischer, Ehud Altman, Immanuel Bloch, and Ulrich Schneider, “Signatures of many-body localization in a controlled open quantum system,” *Phys. Rev. X* **7**, 011034 (2017).
 - [20] Raphaël Bouganne, Manel Bosch Aguilera, Alexis Ghermaoui, Jérôme Beugnon, and Fabrice Gerbier, “Anomalous decay of coherence in a dissipative many-body system,” *Nature Physics* **16**, 21–25 (2020).
 - [21] Iacopo Carusotto and Cristiano Ciuti, “Quantum fluids of light,” *Rev. Mod. Phys.* **85**, 299–366 (2013).
 - [22] Helmut Ritsch, Peter Domokos, Ferdinand Brennecke, and Tilman Esslinger, “Cold atoms in cavity-generated dynamical optical potentials,” *Reviews of Modern Physics* **85**, 553–601 (2013).
 - [23] Sebastian Schmidt and Jens Koch, “Circuit QED lattices: Towards quantum simulation with superconducting circuits,” *Annalen der Physik* **525**, 395–412 (2013).
 - [24] Karyn Le Hur, Loc Henriët, Alexandru Petrescu, Kirill Plekhanov, Guillaume Roux, and Marco Schiró, “Many-body quantum electrodynamics networks: Nonequilibrium condensed matter physics with light,” *Comptes Rendus Physique* **17**, 808 – 835 (2016).
 - [25] Changsuk Noh and Dimitris G. Angelakis, “Quantum simulations and many-body physics with light,” *Reports on Progress in Physics* **80**, 16401 (2017).
 - [26] Michael J. Hartmann, “Quantum simulation with interacting photons,” *Journal of Optics* **18**, 104005 (2016).
 - [27] Heinz Peter Breuer and Francesco Petruccione, *The Theory of Open Quantum Systems*, 1st ed., Vol. 9780199213 (OUP Oxford, 2007).
 - [28] S. Diehl, A. Micheli, A. Kantian, B. Kraus, H. P. Büchler, and P. Zoller, “Quantum states and phases in driven open quantum systems with cold atoms,” *Nature Physics* **4**, 878–883 (2008).
 - [29] Frank Verstraete, Michael M. Wolf, and J. Ignacio Cirac, “Quantum computation and quantum-state engineering driven by dissipation,” *Nature Physics* **5**, 633–636 (2009).
 - [30] K. W. Murch, U. Vool, D. Zhou, S. J. Weber, S. M. Girvin, and I. Siddiqi, “Cavity-assisted quantum bath engineering,” *Physical Review Letters* **109**, 183602 (2012), arXiv:1207.0053.
 - [31] Z. Leghtas, S. Touzard, I. M. Pop, A. Kou, B. Vlastakis, A. Petrenko, K. M. Sliwa, A. Narla, S. Shankar, M. J. Hatridge, M. Reagor, L. Frunzio, R. J. Schoelkopf, M. Mirrahimi, and M. H. Devoret, “Confining the state of light to a quantum manifold by engineered two-photon loss,” *Science* **347**, 853–857 (2015).
 - [32] Sebastian Diehl, Andrea Tomadin, Andrea Micheli, Rosario Fazio, and Peter Zoller, “Dynamical phase transitions and instabilities in open atomic many-body systems,” *Phys. Rev. Lett.* **105**, 015702 (2010).
 - [33] Dario Poletti, Jean-Sébastien Bernier, Antoine Georges, and Corinna Kollath, “Interaction-induced impeding of decoherence and anomalous diffusion,” *Phys. Rev. Lett.* **109**, 045302 (2012).
 - [34] Dario Poletti, Peter Barmettler, Antoine Georges, and Corinna Kollath, “Emergence of glasslike dynamics for dissipative and strongly interacting bosons,” *Phys. Rev. Lett.* **111**, 195301 (2013).
 - [35] Max Ludwig and Florian Marquardt, “Quantum many-body dynamics in optomechanical arrays,” *Phys. Rev. Lett.* **111**, 073603 (2013).
 - [36] L. M. Sieberer, S. D. Huber, E. Altman, and S. Diehl, “Dynamical Critical Phenomena in Driven-Dissipative Systems,” *Physical Review Letters* **110**, 195301 (2013).
 - [37] Jamir Marino and Sebastian Diehl, “Driven markovian quantum criticality,” *Phys. Rev. Lett.* **116**, 070407 (2016).
 - [38] M. Schiró, C. Joshi, M. Bordyuh, R. Fazio, J. Keeling, and H. E. Türeci, “Exotic attractors of the nonequilibrium rabi-hubbard model,” *Phys. Rev. Lett.* **116**, 143603 (2016).
 - [39] Fabrizio Minganti, Alberto Biella, Nicola Bartolo, and Cristiano Ciuti, “Spectral theory of liouvillians for dissipative phase transitions,” *Phys. Rev. A* **98**, 042118 (2018).
 - [40] Riccardo Rota, Fabrizio Minganti, Cristiano Ciuti, and Vincenzo Savona, “Quantum critical regime in a quadratically driven nonlinear photonic lattice,” *Phys. Rev. Lett.* **122**, 110405 (2019).
 - [41] Jeremy T. Young, Alexey V. Gorshkov, Michael Foss-Feig, and Mohammad F. Maghrebi, “Nonequilibrium fixed points of coupled ising models,” *Phys. Rev. X* **10**, 011039 (2020).
 - [42] Andrew J. Daley, “Quantum trajectories and open many-body quantum systems,”

- Advances in Physics **63**, 77–149 (2014), <https://doi.org/10.1080/00018732.2014.933502>.
- [43] F. Verstraete, J. J. García-Ripoll, and J. I. Cirac, “Matrix product density operators: Simulation of finite-temperature and dissipative systems,” *Phys. Rev. Lett.* **93**, 207204 (2004).
 - [44] Michael Zwolak and Guifré Vidal, “Mixed-state dynamics in one-dimensional quantum lattice systems: A time-dependent superoperator renormalization algorithm,” *Phys. Rev. Lett.* **93**, 207205 (2004).
 - [45] Dainius Kilda and Jonathan Keeling, “Fluorescence spectrum and thermalization in a driven coupled cavity array,” *Phys. Rev. Lett.* **122**, 043602 (2019).
 - [46] Augustine Kshetrimayum, Hendrik Weimer, and Román Orús, “A simple tensor network algorithm for two-dimensional steady states,” *Nature Communications* **8**, 1291 (2017).
 - [47] Haggai Landa, Marco Schiró, and Grégoire Misguich, “Multistability of driven-dissipative quantum spins,” *Phys. Rev. Lett.* **124**, 043601 (2020).
 - [48] S. Finazzi, A. Le Boité, F. Storme, A. Baksic, and C. Ciuti, “Corner-space renormalization method for driven-dissipative two-dimensional correlated systems,” *Phys. Rev. Lett.* **115**, 080604 (2015).
 - [49] Hendrik Weimer, “Variational principle for steady states of dissipative quantum many-body systems,” *Phys. Rev. Lett.* **114**, 040402 (2015).
 - [50] Jiasen Jin, Alberto Biella, Oscar Viyuela, Leonardo Mazza, Jonathan Keeling, Rosario Fazio, and Davide Rossini, “Cluster mean-field approach to the steady-state phase diagram of dissipative spin systems,” *Phys. Rev. X* **6**, 031011 (2016).
 - [51] L M Sieberer, M Buchholdt, and S Diehl, “Keldysh field theory for driven open quantum systems,” *Reports on Progress in Physics* **79**, 096001 (2016).
 - [52] Matteo Biondi, Saskia Lienhard, Gianni Blatter, Hakan E Treci, and Sebastian Schmidt, “Spatial correlations in driven-dissipative photonic lattices,” *New Journal of Physics* **19**, 125016 (2017).
 - [53] Filippo Vicentini, Fabrizio Minganti, Riccardo Rota, Giuliano Orso, and Cristiano Ciuti, “Critical slowing down in driven-dissipative bose-hubbard lattices,” *Phys. Rev. A* **97**, 013853 (2018).
 - [54] Hendrik Weimer, Augustine Kshetrimayum, and Román Orús, “Simulation methods for open quantum many-body systems,” *arXiv e-prints*, arXiv:1907.07079 (2019), arXiv:1907.07079 [quant-ph].
 - [55] Filippo Vicentini, Alberto Biella, Nicolas Regnault, and Cristiano Ciuti, “Variational neural-network ansatz for steady states in open quantum systems,” *Phys. Rev. Lett.* **122**, 250503 (2019).
 - [56] Nobuyuki Yoshioka and Ryusuke Hamazaki, “Constructing neural stationary states for open quantum many-body systems,” *Phys. Rev. B* **99**, 214306 (2019).
 - [57] Alexandra Nagy and Vincenzo Savona, “Variational quantum monte carlo method with a neural-network ansatz for open quantum systems,” *Phys. Rev. Lett.* **122**, 250501 (2019).
 - [58] Michael J. Hartmann and Giuseppe Carleo, “Neural-network approach to dissipative quantum many-body dynamics,” *Phys. Rev. Lett.* **122**, 250502 (2019).
 - [59] Antoine Georges, Gabriel Kotliar, Werner Krauth, and Marcelo J. Rozenberg, “Dynamical mean-field theory of strongly correlated fermion systems and the limit of infinite dimensions,” *Reviews of Modern Physics* **68**, 13–125 (1996).
 - [60] Krzysztof Byczuk and Dieter Vollhardt, “Correlated bosons on a lattice: Dynamical mean-field theory for bose-einstein condensed and normal phases,” *Phys. Rev. B* **77**, 235106 (2008).
 - [61] Peter Anders, Emanuel Gull, Lode Pollet, Matthias Troyer, and Philipp Werner, “Dynamical mean field solution of the bose-hubbard model,” *Phys. Rev. Lett.* **105**, 096402 (2010).
 - [62] Walter Metzner and Dieter Vollhardt, “Correlated Lattice Fermions in Infinite Dimensions,” *Physical Review Letters* **62**, 324–327 (1989).
 - [63] Antoine Georges and Gabriel Kotliar, “Hubbard model in infinite dimensions,” *Physical Review B* **45**, 6479–6483 (1992).
 - [64] Hideo Aoki, Naoto Tsuji, Martin Eckstein, Marcus Kollar, Takashi Oka, and Philipp Werner, “Nonequilibrium dynamical mean-field theory and its applications,” *Reviews of Modern Physics* **86**, 779–837 (2014).
 - [65] Enrico Arrigoni, Michael Knap, and Wolfgang von der Linden, “Nonequilibrium dynamical mean-field theory: An auxiliary quantum master equation approach,” *Phys. Rev. Lett.* **110**, 086403 (2013).
 - [66] Hugo U. R. Strand, Martin Eckstein, and Philipp Werner, “Nonequilibrium dynamical mean-field theory for bosonic lattice models,” *Physical Review X* **5**, 11038 (2015).
 - [67] Tony E. Lee and H. R. Sadeghpour, “Quantum Synchronization of Quantum van der Pol Oscillators with Trapped Ions,” *Physical Review Letters* **111**, 234101 (2013).
 - [68] Niels Lörch, Ehud Amitai, Andreas Nunnenkamp, and Christoph Bruder, “Genuine Quantum Signatures in Synchronization of Anharmonic Self-Oscillators,” *Physical Review Letters* **117**, 073601 (2016).
 - [69] Stefan Walter, Andreas Nunnenkamp, and Christoph Bruder, “Quantum Synchronization of a Driven Self-Sustained Oscillator,” *Physical Review Letters* **112**, 094102 (2014).
 - [70] Stefan Walter, Andreas Nunnenkamp, and Christoph Bruder, “Quantum synchronization of two Van der Pol oscillators,” *Annalen der Physik* **527**, 131–138 (2015).
 - [71] Alexandre Roulet and Christoph Bruder, “Synchronizing the Smallest Possible System,” *Physical Review Letters* **121**, 053601 (2018).
 - [72] Alexandre Roulet and Christoph Bruder, “Quantum Synchronization and Entanglement Generation,” *Physical Review Letters* **121**, 063601 (2018).
 - [73] Shovan Dutta and Nigel R. Cooper, “Critical Response of a Quantum van der Pol Oscillator,” *Physical Review Letters* **123**, 250401 (2019).
 - [74] Gian Luca Giorgi, Fernando Galve, Gonzalo Manzano, Pere Colet, and Roberta Zambrini, “Quantum correlations and mutual synchronization,” *Physical Review A* **85**, 052101 (2012).
 - [75] Gonzalo Manzano, Fernando Galve, Gian Luca Giorgi, Emilio Hernández-García, and Roberta Zambrini, “Synchronization, quantum correlations and entanglement in oscillator networks,” *Scientific Reports* **3**, 1–6 (2013).
 - [76] Guo-jian Qiao, Hui-xia Gao, Hao-di Liu, and X. X. Yi, “Quantum synchronization of two mechanical oscillators in coupled optomechanical systems with Kerr

- nonlinearity,” *Scientific Reports* **8**, 1–11 (2018).
- [77] Sameer Sonar, Michal Hajdušek, Manas Mukherjee, Rosario Fazio, Vlatko Vedral, Sai Vinjanampathy, and Leong-Chuan Kwek, “Squeezing enhances quantum synchronization,” *Phys. Rev. Lett.* **120**, 163601 (2018).
- [78] Noufal Jaseem, Michal Hajdušek, Vlatko Vedral, Rosario Fazio, Leong-Chuan Kwek, and Sai Vinjanampathy, “Quantum synchronization in nanoscale heat engines,” *Phys. Rev. E* **101**, 020201 (2020).
- [79] J. Tindall, C. Sánchez Muñoz, B. Buča, and D. Jaksch, “Quantum synchronisation enabled by dynamical symmetries and dissipation,” *New Journal of Physics* **22**, 013026 (2020).
- [80] Matthew P.A. Fisher, Peter B. Weichman, G. Grinstein, and Daniel S. Fisher, “Boson localization and the superfluid-insulator transition,” *Physical Review B* **40**, 546–570 (1989).
- [81] Marco Schiro and Orazio Scarlatella, “Quantum impurity models coupled to Markovian and non-Markovian baths,” *The Journal of Chemical Physics* **151**, 044102 (2019).
- [82] Michael J. Hartmann, Fernando G. S. L. Brandão, and Martin B. Plenio, “Strongly interacting polaritons in coupled arrays of cavities,” *Nature Physics* **2**, 849–855 (2006).
- [83] Dimitris G. Angelakis, Marcelo Franca Santos, and Sougato Bose, “Photon-blockade-induced mott transitions and xy spin models in coupled cavity arrays,” *Phys. Rev. A* **76**, 031805 (2007).
- [84] Michael J. Hartmann, “Polariton crystallization in driven arrays of lossy nonlinear resonators,” *Phys. Rev. Lett.* **104**, 113601 (2010).
- [85] Jiasen Jin, Davide Rossini, Rosario Fazio, Martin Leib, and Michael J. Hartmann, “Photon solid phases in driven arrays of nonlinearly coupled cavities,” *Phys. Rev. Lett.* **110**, 163605 (2013).
- [86] Alexandre Le Boité, Giuliano Orso, and Cristiano Ciuti, “Steady-state phases and tunneling-induced instabilities in the driven dissipative bose-hubbard model,” *Phys. Rev. Lett.* **110**, 233601 (2013).
- [87] José Lebreuilly, Alberto Biella, Florent Storme, Davide Rossini, Rosario Fazio, Cristiano Ciuti, and Iacopo Carusotto, “Stabilizing strongly correlated photon fluids with non-markovian reservoirs,” *Phys. Rev. A* **96**, 033828 (2017).
- [88] M. Foss-Feig, P. Niroula, J. T. Young, M. Hafezi, A. V. Gorshkov, R. M. Wilson, and M. F. Maghrebi, “Emergent equilibrium in many-body optical bistability,” *Phys. Rev. A* **95**, 043826 (2017).
- [89] Matteo Biondi, Gianni Blatter, Hakan E. Treci, and Sebastian Schmidt, “Nonequilibrium gas-liquid transition in the driven-dissipative photonic lattice,” *Phys. Rev. A* **96**, 043809 (2017).
- [90] Orazio Scarlatella, Rosario Fazio, and Marco Schiró, “Emergent finite frequency criticality of driven-dissipative correlated lattice bosons,” *Phys. Rev. B* **99**, 064511 (2019).
- [91] V. V. Dodonov and S. S. Mizrahi, “Exact stationary photon distributions due to competition between one- and two-photon absorption and emission,” *Journal of Physics A: Mathematical and General* **30**, 5657–5667 (1997).
- [92] M. Dykman, “Heating and cooling of local and quasilocal vibrations by a nonresonance field.pdf,” *Sov. phys. Solid State* **20**, 1306–1311 (1978).
- [93] We are not limited to the coordination numbers we spanned in Fig. 2 and we can run Open-DMFT equations for smaller values of z , but computing the phase diagram becomes particularly challenging, as it moves towards higher drive-to-loss r values, as shown in Fig. 2, which are numerically hard to access requiring bigger Hilbert space sizes.
- [94] Berislav Buča, Joseph Tindall, and Dieter Jaksch, “Non-stationary coherent quantum many-body dynamics through dissipation,” *Nature Communications* **10**, 1804.06744 (2019).
- [95] F. Iemini, A. Russomanno, J. Keeling, M. Schiró, M. Dalmonte, and R. Fazio, “Boundary time crystals,” *Phys. Rev. Lett.* **121**, 035301 (2018).
- [96] Steven H. Strogatz and Renato E. Mirollo, “Stability of incoherence in a population of coupled oscillators,” *Journal of Statistical Physics* **63**, 613–635 (1991).
- [97] Paul C. Matthews, Renato E. Mirollo, and Steven H. Strogatz, “Dynamics of a large system of coupled nonlinear oscillators,” *Physica D: Nonlinear Phenomena* **52**, 293–331 (1991).
- [98] M. C. Cross, A. Zumdieck, Ron Lifshitz, and J. L. Rogers, “Synchronization by Nonlinear Frequency Pulling,” *Physical Review Letters* **93**, 224101 (2004).
- [99] Orazio Scarlatella, Aashish A. Clerk, and Marco Schiró, “Spectral functions and negative density of states of a driven-dissipative nonlinear quantum resonator,” *New Journal of Physics* **21**, 043040 (2018).
- [100] Marc Antoine Lemonde, Nicolas Didier, and Aashish A. Clerk, “Nonlinear interaction effects in a strongly driven optomechanical cavity,” *Physical Review Letters* **111**, 53602 (2013).
- [101] B. A. Levitan, A. Metelmann, and A. A. Clerk, “Optomechanics with two-phonon driving,” *New Journal of Physics* **18**, 93014 (2016).
- [102] Alex Kamenev, *Field theory of non-equilibrium systems* (Cambridge University Press, 2011).
- [103] Emanuel Gull, Andrew J. Millis, Alexander I. Lichtenstein, Alexey N. Rubtsov, Matthias Troyer, and Philipp Werner, “Continuous-time monte carlo methods for quantum impurity models,” *Rev. Mod. Phys.* **83**, 349–404 (2011).
- [104] Lothar Mühlbacher and Eran Rabani, “Real-time path integral approach to nonequilibrium many-body quantum systems,” *Physical Review Letters* **100**, 176403 (2008).
- [105] Marco Schiró and Michele Fabrizio, “Real-time diagrammatic Monte Carlo for nonequilibrium quantum transport,” *Phys. Rev. B* **79**, 153302 (2009).
- [106] Philipp Werner, Takashi Oka, and Andrew J. Millis, “Diagrammatic Monte Carlo simulation of nonequilibrium systems,” *Physical Review B - Condensed Matter and Materials Physics* **79**, 35320 (2009).
- [107] Rosario E.V. Profumo, Christoph Groth, Laura Mesio, Olivier Parcollet, and Xavier Waintal, “Quantum Monte Carlo for correlated out-of-equilibrium nanoelectronic devices,” *Physical Review B - Condensed Matter and Materials Physics* **91**, 245154 (2015).
- [108] Guy Cohen, Emanuel Gull, David R. Reichman, and Andrew J. Millis, “Taming the Dynamical Sign Problem in Real-Time Evolution of Quantum Many-Body Problems,” *Physical Review Letters* **115**, 266802 (2015).
- [109] N. E. Bickers, *Review of Techniques in the Large-N Ex-*

- pansion for Dilute Magnetic Alloys*, Tech. Rep. (1987) publication Title: Reviews of Modern Physics.
- [110] Peter Nordlander, Michael Pustilnik, Yigal Meir, Ned S. Wingreen, and David C. Langreth, “How Long Does It Take for the Kondo Effect to Develop?” *Physical Review Letters* **83**, 808–811 (1999).
 - [111] Martin Eckstein and Philipp Werner, “Nonequilibrium dynamical mean-field calculations based on the non-crossing approximation and its generalizations,” *Physical Review B - Condensed Matter and Materials Physics* **82**, 115115 (2010).
 - [112] Andreas Rüegg, Emanuel Gull, Gregory A. Fiete, and Andrew J. Millis, “Sum rule violation in self-consistent hybridization expansions,” *Physical Review B - Condensed Matter and Materials Physics* **87**, 75124 (2013).
 - [113] Francesco Peronaci, Marco Schiró, and Olivier Parcollet, “Resonant Thermalization of Periodically Driven Strongly Correlated Electrons,” *Physical Review Letters* **120**, 197601 (2018).
 - [114] Francesco Peronaci, Olivier Parcollet, and Marco Schiró, “Enhancement of local pairing correlations in periodically driven mott insulators,” *Phys. Rev. B* **101**, 161101 (2020).
 - [115] Enrico Arrigoni, Michael Knap, and Wolfgang Von Der Linden, “Nonequilibrium dynamical mean-field theory: An auxiliary quantum master equation approach,” *Physical Review Letters* **110**, 86403 (2013).
 - [116] Hugo U. R. Strand, Martin Eckstein, and Philipp Werner, “Beyond the Hubbard bands in strongly correlated lattice bosons,” *Physical Review A - Atomic, Molecular, and Optical Physics* **92**, 63602 (2015).
 - [117] Herbert Schoeller and Gerd Schön, “Mesoscopic quantum transport: Resonant tunneling in the presence of a strong coulomb interaction,” *Phys. Rev. B* **50**, 18436–18452 (1994).
 - [118] Marco Schiró, “Real-time dynamics in quantum impurity models with diagrammatic Monte Carlo,” *Physical Review B - Condensed Matter and Materials Physics* **81**, 85126 (2010).
 - [119] R Alicki, “The quantum open system as a model of the heat engine,” *Journal of Physics A: Mathematical and General* **12**, L103–L107 (1979).
 - [120] Tova Feldmann and Ronnie Kosloff, “Quantum four-stroke heat engine: Thermodynamic observables in a model with intrinsic friction,” *Phys. Rev. E* **68**, 016101 (2003).
 - [121] Ángel Rivas, “Strong coupling thermodynamics of open quantum systems,” *Phys. Rev. Lett.* **124**, 160601 (2020).
 - [122] H. E. D. Scovil and E. O. Schulz-DuBois, “Three-level masers as heat engines,” *Phys. Rev. Lett.* **2**, 262–263 (1959).
 - [123] E. Boukobza and D. J. Tannor, “Thermodynamic analysis of quantum light amplification,” *Phys. Rev. A* **74**, 063822 (2006).
 - [124] E. Boukobza and D. J. Tannor, “Three-level systems as amplifiers and attenuators: A thermodynamic analysis,” *Phys. Rev. Lett.* **98**, 240601 (2007).
 - [125] Y.-Y. Liu, J. Stehlik, C. Eichler, M. J. Gullans, J. M. Taylor, and J. R. Petta, “Semiconductor double quantum dot micromaser,” *Science* **347**, 285–287 (2015), <https://science.sciencemag.org/content/347/6219/285.full.pdf>
 - [126] José Lebreuilly, Michiel Wouters, and Iacopo Carusotto, “Towards strongly correlated photons in arrays of dissipative nonlinear cavities under a frequency-dependent incoherent pumping,” *Comptes Rendus Physique* **17**, 836–860 (2016).
 - [127] M. Cross and P. Hohenberg, “Pattern formation outside of equilibrium,” *Rev. Mod. Phys.* **65**, 851–1112 (1993).
 - [128] Victor V. Albert and Liang Jiang, “Symmetries and conserved quantities in lindblad master equations,” *Phys. Rev. A* **89**, 022118 (2014).
 - [129] Tony E. Lee, H. Hffner, and M. C. Cross, “Antiferromagnetic phase transition in a nonequilibrium lattice of Rydberg atoms,” *Phys. Rev. A* **84**, 031402 (2011).
 - [130] Ching-Kit Chan, Tony E. Lee, and Sarang Gopalakrishnan, “Limit-cycle phase in driven-dissipative spin systems,” *Phys. Rev. A* **91**, 051601 (2015).
 - [131] Ryan M. Wilson, Khan W. Mahmud, Anzi Hu, Alexey V. Gorshkov, Mohammad Hafezi, and Michael Foss-Feig, “Collective phases of strongly interacting cavity photons,” *Phys. Rev. A* **94**, 033801 (2016).
 - [132] E. T. Owen, J. Jin, D. Rossini, R. Fazio, and M. J. Hartmann, “Quantum correlations and limit cycles in the driven-dissipative Heisenberg lattice,” *New Journal of Physics* **20**, 045004 (2018).
 - [133] Peter Degenfeld-Schonburg and Michael J. Hartmann, “Self-consistent projection operator theory for quantum many-body systems,” *Physical Review B - Condensed Matter and Materials Physics* **89**, 245108 (2014).
 - [134] Aditi Mitra, So Takei, Yong Baek Kim, and A. J. Millis, “Nonequilibrium quantum criticality in open electronic systems,” *Phys. Rev. Lett.* **97**, 236808 (2006).
 - [135] A. A. Clerk, M. H. Devoret, S. M. Girvin, Florian Marquardt, and R. J. Schoelkopf, “Introduction to quantum noise, measurement, and amplification,” *Reviews of Modern Physics* **82**, 1155–1208 (2010).
 - [136] Laura Foini, Leticia F. Cugliandolo, and Andrea Gambassi, “Fluctuation-dissipation relations and critical quenches in the transverse field ising chain,” *Phys. Rev. B* **84**, 212404 (2011).
 - [137] Emanuele G. Dalla Torre, Eugene Demler, Thierry Giamarchi, and Ehud Altman, “Dynamics and universality in noise-driven dissipative systems,” *Phys. Rev. B* **85**, 184302 (2012).
 - [138] Marco Schiró and Aditi Mitra, “Transient orthogonality catastrophe in a time-dependent nonequilibrium environment,” *Phys. Rev. Lett.* **112**, 246401 (2014).
 - [139] Steven H. Strogatz and Renato E. Mirollo, “Stability of incoherence in a population of coupled oscillators,” *Journal of Statistical Physics* **63**, 613–635 (1991).
 - [140] Roland Lauter, Aditi Mitra, and Florian Marquardt, “From kardar-parisi-zhang scaling to explosive desynchronization in arrays of limit-cycle oscillators,” *Phys. Rev. E* **96**, 012220 (2017).
 - [141] Julio T. Barreiro, Markus Müller, Philipp Schindler, Daniel Nigg, Thomas Monz, Michael Chwalla, Markus Hennrich, Christian F. Roos, Peter Zoller, and Rainer Blatt, “An open-system quantum simulator with trapped ions,” *Nature* **470**, 486–491 (2011).
 - [142] Tony E. Lee, Sarang Gopalakrishnan, and Mikhail D. Lukin, “Unconventional magnetism via optical pumping of interacting spin systems,” *Phys. Rev. Lett.* **110**, 257204 (2013).
 - [143] Elmar Haller, James Hudson, Andrew Kelly, Dylan A. Cotta, Bruno Peaudecerf, Graham D. Bruce, and Stefan Kuhr, “Single-atom imaging of fermions in a

- quantum-gas microscope,” *Nature Physics* **11**, 738–742 (2015).
- [144] Kazuki Yamamoto, Masaya Nakagawa, Kyosuke Adachi, Kazuaki Takasan, Masahito Ueda, and Norio Kawakami, “Theory of non-hermitian fermionic superfluidity with a complex-valued interaction,” *Phys. Rev. Lett.* **123**, 123601 (2019).
- [145] Masaya Nakagawa, Naoto Tsuji, Norio Kawakami, and Masahito Ueda, “Dynamical sign reversal of magnetic correlations in dissipative hubbard models,” *Phys. Rev. Lett.* **124**, 147203 (2020).